

INVESTIGATION OF THE DYNAMIC MEMBRANE TOPOLOGY OF BCL-2

**INVESTIGATING THE DYNAMIC MEMBRANE TOPOLOGY
OF THE ANTI-APOPTOTIC PROTEIN, BCL-2,
USING CYSTEINE SCANNING MUTAGENESIS**

By

GWENDOLYN JANE ROBERTS, B. Sc.

A Thesis

Submitted to the School of Graduate Studies

in Partial Fulfillment of the Requirements

for the Degree

Master of Science

McMaster University

©Copyright by Gwendolyn Jane Roberts, August 2005

MASTER OF SCIENCE (2005)
(Biochemistry and Biomedical Sciences)

McMaster University
Hamilton, Ontario, Canada

TITLE: Investigating the Dynamic Membrane Topology
Of the Anti-Apoptotic Protein, Bcl-2, Using Cysteine Scanning
Mutagenesis

AUTHOR: Gwendolyn Jane Roberts, B.Sc. (Queen's University)

SUPERVISOR: Dr David W. Andrews

NUMBER OF PAGES: xii, 89

ABSTRACT

Bcl-2 proteins play a critical role in the regulation of apoptosis, a form of programmed cell death. Apoptosis is important during development to facilitate the elimination of supernumerary, damaged or harmful cells in multicellular organisms. Altered regulation of apoptosis is associated with many diseases such as several forms of cancer as well as autoimmune and degenerative disorders. The way in which Bcl-2 proteins regulate apoptosis is unknown and much research is focused on elucidating the molecular mechanism of their function. Bcl-2, an anti-apoptotic member of this family, is localized to the mitochondria, endoplasmic reticulum and nuclear envelope. In healthy cells, Bcl-2 adopts a typical tail-anchored topology in which the carboxyl-terminal helix ($\alpha 9$) is inserted into the membrane, anchoring the protein, leaving the majority of the protein in the cytosol. Previous results from our lab have shown that after the induction of apoptosis, Bcl-2 undergoes a conformational change in which the endogenous cysteine residue, C158, in the $\alpha 5$ helix becomes protected from a membrane impermeant cysteine specific labelling reagent, IASD (4-acetamido-4'-((iodoacetyl)amino)-stilbene-2,2'-disulfonate). Modification of cysteine residues results in a change in migration of Bcl-2 in an isoelectric focusing, IEF, gel system. To investigate the nature of this conformational change, cysteine scanning mutagenesis was used to determine the topology of Bcl-2 in the late stages of apoptosis. The results from the current study showed that in rat 1 myc ERTM fibroblasts, a discontinuous sequence of residues in the $\alpha 5$ and $\alpha 6$ helices of Bcl-2 become protected from IASD labelling after the induction of apoptosis by etoposide or serum starvation. The data support a model topology in which,

during apoptosis, Bcl-2 undergoes a functionally significant conformational change, going from a single spanning transmembrane protein to a polytopic membrane protein in which three helices span the membrane, $\alpha 5$, $\alpha 6$ and $\alpha 9$.

To My Birch Island Family

ACKNOWLEDGEMENTS

I would like to thank my Supervisor Dr David Andrews for giving me this opportunity and for helping me to achieve my goals. I would also like to thank my committee members Dr Brian Leber and Dr Bernardo Trigatti for challenging and advising me throughout this project. To the members of the Andrew's Lab, past and present, thank you for all your support and for making my time there so memorable! In particular I would like to thank Felicia for the good advice, walks and tea. To Weijia, I give my thanks for the hours of help in tissue culture and for her always smiling face. To Matt, the best bay-mate you could ask for, thank you for the guidance, laughter and keeping me on my toes. To Paulina, Lieven, Matthew and Steve, thank you for all the intense coffee room discussions and good times at the Phoenix. I also want to thank Suzanne Lapolla for making the Bcl-2 mutant plasmid constructs and Valerie for helping me to screen one of my many sets of mutants. This thesis would not be possible if it were not for my family. To my Mum and Dad, thank you for the unwavering support. Thanks to my brother for systematically bringing me back to reality. Last but not least, thanks to Gab, for everything that cannot be described in words! Look how far we have come!

TABLE OF CONTENTS

	Page
Abstract	iii
Acknowledgements	vi
Table of Contents	vii
Table of Figures	ix
Table of Tables	x
Table of Abbreviations	xii
Chapter 1: Introduction	1
1.1 Apoptosis	1
1.2 The Bcl-2 Protein Family	1
1.3 Apoptotic Pathways	4
Induction of Apoptosis	4
Caspases and Other Factors involved in Apoptosis	8
1.4 The Molecular Mechanism of Bcl-2	10
1.5 The Structure of Bcl-2	11
1.6 The Dynamic Membrane Topology of Bcl-2	14
Chapter 2: Materials and Methods	20
2.1 General Materials	20
2.2 Antibodies	20
2.3 General Methods	21
2.3.1 Plasmids and Proteins	21
2.3.2 Transcription and translation	28
2.3.3 Microsome Targeting	29
2.3.4 Tissue Cell Culture	31
2.3.5 Transfection and Retroviral Infection of Rat 1 myc ERTM fibroblasts	31
2.3.6 Cell Death Assays	34

2.3.7 Preparation of Whole Cell Lysates	34
2.3.8 Preparation of Subcellular fractions from Cell Extracts by Nitrogen Cavitation	35
2.3.9 Protein Sample Quantification	35
2.3.10 Protein Electrophoresis	36
2.3.11 Immunoblotting	37
2.3.12 IASD Labelling Reactions	38
2.3.13 Optimization of the Resolution of the Band Shift Associated with IASD Labelled Bcl-2 using an Isoelectric Focusing Gel System	42
2.3.14 Quantification of Western Blots	46
Chapter 3: Results	48
3.1 Expression of Bcl-2 mutants in rat 1 myc ERTM fibroblasts after retroviral infection	48
3.2 Bcl-2 mutant proteins expressed in rat 1 myc ERTM fibroblasts exhibit anti-apoptotic function	52
3.3 Bcl-2 membrane topology after apoptosis, assayed by IASD labelling of single cysteine mutants	60
3.4 IASD labelling data suggests that Bcl-2 changes conformation after the induction of apoptosis, whereby helices $\alpha 5$ and $\alpha 6$ insert into the membrane	74
Chapter 4: Discussion	78
4.1 Expression of Bcl-2 mutant proteins	78
4.2 Anti-apoptotic function of Bcl-2 Mutants	79
4.3 Change in membrane topology of Bcl-2 during apoptosis	82
4.4 Functional Significance of the change in topology of Bcl-2 during apoptosis	84
4.5 Conclusion	89
Chapter 5: References	90

TABLE OF FIGURES

	Page
Chapter 1: Introduction	
Figure 1.1 The Bcl-2 Family of Proteins	3
Figure 1.2. The Two Main Pathways of Apoptosis.	7
Figure 1.3 The Amino Acid Sequence, Hydropathy plot, NMR Structure and Schematic Representation of Bcl-2	12
Figure 1.4 The Membrane Impermeant, Cysteine Specific Labelling Reagent, IASD, Used to Determine the Membrane Topology of Bcl-2	16
Chapter 2: Materials and Methods	
Figure 2.1 Plasmid maps of the pRC/CMV Bcl-2, pBABE hygro and pBABE hygro Bcl-2 vectors	23
Figure 2.2 Microsome targeting assay using [³⁵ S]-Methionine labelled wild type Bcl-2 and single cysteine mutants	30
Figure 2.3 Expression of Bcl-2 C158V/C229V mutant proteins in rat 1 myc ERTM fibroblasts	33
Figure 2.4 IASD labelling of Bcl-xL	40
Figure 2.5 Optimization of the isoelectric focusing gel system to resolve the band shift associated with IASD labelled Bcl-2	45
Chapter 3: Results	
Figure 3.1 Position of the Bcl-2 C158A, C229V single cysteine mutants	50
Figure 3.2 Expression of Bcl-2 mutant proteins in rat 1 myc ERTM fibroblasts after retroviral infection	51
Figure 3.3 Anti-apoptotic function of Bcl-2 mutant proteins in rat 1 myc ERTM fibroblasts after treatment with etoposide or serum starvation	53
Figure 3.4 Isoelectric focusing of IASD labelled wild type and mutant Bcl-2 proteins in untreated, etoposide- or serum starvation-treated cells	63
Figure 3.5 Schematic representations of residues which are protected from IASD labelling after etoposide or serum starvation treatment and models of predicted membrane topology	75

TABLE OF TABLES

	Page
Chapter 2: Materials and Methods	
Table 1 Mutant Bcl-2 proteins used for membrane topology analysis and their corresponding DW Andrews laboratory plasmid numbers	25
Table 2 Mutant Bcl-2 C158V/C229V proteins obtained from Dr J Lin not used for membrane topology analysis and their corresponding DW Andrews laboratory plasmid numbers	26
Table 3 Mutant Bcl-2 proteins designed to disrupt dimerization obtained from Dr J Lin and their corresponding DW Andrews laboratory plasmid numbers	28
Chapter 3: Results	
Table 4 One-way ANOVA comparing PARP cleavage after 12 hours of etoposide treatment	56
Table 5 One-way ANOVA comparing PARP cleavage after 18 hours of etoposide treatment	57
Table 6 One-way ANOVA comparing PARP cleavage after 24 hours in serum starvation conditions	58
Table 7 One-way ANOVA comparing PARP cleavage after 48 hours in serum starvation conditions	59
Table 8 One-way ANOVA comparing protection from IASD labelling of wild type and Bcl-2 mutant proteins in untreated cells	68
Table 9 One-way ANOVA comparing protection from IASD labelling of wild type and Bcl-2 mutant proteins after 18 hours of etoposide treatment	69
Table 10 One-way ANOVA comparing protection from IASD labelling of wild type and Bcl-2 mutant proteins after 48 hours of serum starvation	70
Table 11 One-way ANOVA comparing the <u>net</u> protection from IASD labelling of wild type and mutant Bcl-2 proteins in untreated cells, and after 18 hours of etoposide treatment	71
Table 12 One-way ANOVA comparing the <u>net</u> protection from IASD labelling of wild type and mutant Bcl-2 proteins in untreated cells, and after 48 hours	72

of serum starvation

Table 13 Summary of the degree of anti-apoptotic function and protection from IASD labelling in wild type and Bcl-2 mutants	73
--	----

TABLE OF ABBREVIATIONS

AIF	Apoptosis inducing factor
Apaf-1	Apoptosis protease-activating factor-1
Bak	Bcl-2 agonist killer
Bax	Bcl-2-associated protein X
Bcl-2	B-cell lymphoma protein 2
BH	Bcl-2 homologous
Bid	BH3 interacting domain death agonist
BSA	Bovine serum albumin
CHAPS	3-[(3-chloroamidopropyl)dimethylammonio]-1-propane-sulfonate
DISC	death-inducing signalling complex
DTT	Dithiothreitol
ECL	Enhanced Chemiluminescence
EGF	Epidermal growth factor
ER	Endoplasmic reticulum
FADD	Fas-associated death domain protein
FBS	Fetal bovine serum
HRP	Horseradish-peroxidase
IAP	Inhibitors of apoptosis protein
IASD	4-acetamido-4'-((iodoacetyl)amino)-stilbene-2,2'-disulfonic acid
IEF	Isoelectric focusing
IGEPAL-630	Nonylphenyl-polyethylenglycol (formally known as NP-40)
MMP	Mitochondrial membrane permeabilization
PARP	Poly (ADP- ribose) polymerase
PBS	Phosphate buffered saline
PDGF	Platelet-derived growth factor
PEI	Polyethylenimine
pI	Isoelectric point
PI3K	Phosphatidylinositol 3-kinase

PVDF	Poly vinylidene difluoride
SDS	Sodium dodecyl sulfate
PAGE	Polyacrylamide-gel electrophoresis
SMAC/DIABLO	Second mitochondria-derived activator of caspase/direct IAP binding protein with low pI
tBid	Truncated Bid
TLB	Tricine loading buffer
TM	Transmembrane
TNF	Tumour Necrosis Factor
TRAIL-R1	TNF-related-apoptosis-inducing-ligand-R1

CHAPTER 1: INTRODUCTION

1.1 Apoptosis

Apoptosis is a form of programmed cell death which facilitates the elimination of supernumerary, damaged or harmful cells from multicellular organisms. Apoptosis was first described in 1972 by Kerr, Wyllie and Currie in reference to cells that systematically shrink and bleb, as chromatin condenses and internucleosomal DNA is cleaved in an orderly fashion (Kerr et al., 1972). Cellular contents are then packaged into vesicles and engulfed by other cells. This process is essential for developmental morphogenesis and tissue homeostasis, as well as for defence against pathogens (Adams and Cory, 1998).

Apoptosis is a highly regulated process, involving many proteins and associated factors. Altered regulation of apoptosis is associated with many diseases such as cancer as well as autoimmune and degenerative disorders. In cancer, apoptosis is often impaired thereby allowing cells to live in adverse conditions. This irregular cell death response interferes with certain cancer therapeutics such as chemotherapy and γ -radiation which kill target cells primarily through the induction of apoptosis (Cory and Adams, 2002). Research into the mechanism of apoptosis is essential for designing new treatments for these apoptosis-resistant cells.

1.2 The Bcl-2 Protein Family

The critical regulators of apoptosis are the Bcl-2 family of proteins, individual members of which either inhibit or promote cell death. Altered regulation of these proteins is commonly found in cancer. The initial identification of the protein Bcl-2, for

which the family is named, came in 1985 by Tsujimoto and his colleagues who identified a novel protein upregulated in follicular B-cell lymphoma and named it Bcl-2 for B-cell lymphoma protein 2. An error during immunoglobulin chromosomal translocation at the pre-B-cell stage of differentiation causes the Bcl-2 gene to be placed in close proximity to the powerful immunoglobulin gene complex enhancer, thereby causing deregulated expression of Bcl-2 (Tsujimoto et al., 1985). Further investigation demonstrated that Bcl-2 had a unique function for an oncogene in that its expression did not promote proliferation but rather inhibited cell death (Vaux et al., 1988). The elucidation of the function of the Bcl-2 protein led to the understanding that impaired apoptosis is a crucial component in tumourigenesis (Cory et al., 1999).

Since 1985, at least twenty proteins with varying homology to Bcl-2 have been identified. Pro- and anti-apoptotic Bcl-2 family members work together to determine the fate of a cell. The exact mechanism of action of the Bcl-2 proteins in apoptosis is largely unknown. Each family member contains up to four Bcl-2 homologous, BH, regions (Diaz et al., 1997; Petros et al., 2004). The anti-apoptotic members, such as Bcl-2 and Bcl-xL, contain all four of the BH regions, BH1-BH4 (Figure 1.1). The pro-apoptotic members are divided into two groups, those with multiple BH regions, BH1-BH3, such as Bax and Bak and those with BH3 regions only, such as Bid or Bim.

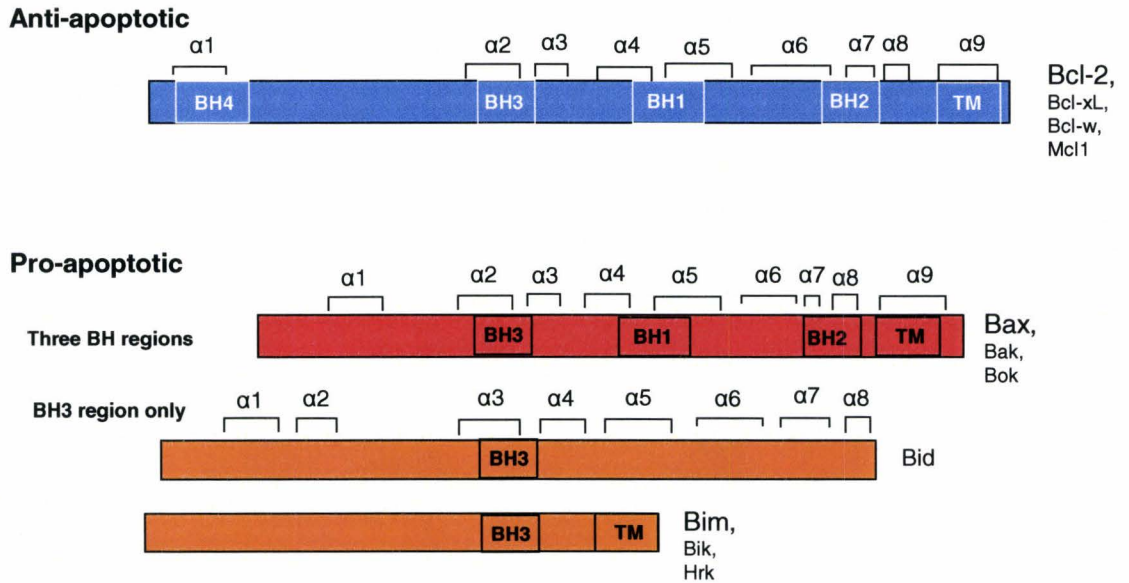


Figure 1.1 The Bcl-2 Family of Proteins. This family consists of anti- and pro-apoptotic members that share various combinations of BH (Bcl-2 homologous) regions. The schematic diagrams show representative members from each of the categories (labelled in bold on the right). Examples of other members of each group are also listed. BH regions and α helices are indicated. Several members contain transmembrane (TM) regions which allow interaction with intracellular membranes (adapted from (Cory and Adams, 2002).

1.3 Apoptotic Pathways

Induction of Apoptosis

The initiation of apoptosis occurs through two alternative pathways: the extrinsic pathway, mediated by death receptors at the cell surface and the intrinsic pathway in which death signals are received at the level of the mitochondria. Both pathways are mediated by activated caspases and are regulated by the Bcl-2 family of proteins; they converge at the level of the mitochondria and share common characteristic events (Igney and Krammer, 2002) (Figure 1.2).

Death receptors are a subset of proteins within the Tumour Necrosis Factor (TNF) receptor family. These proteins contain an extracellular domain characterised by a sequence of 2-5 cysteine-rich repeats as well as an intracellular 'death domain' (Bratton et al., 2000). Members of this subfamily include CD95 (APO/Fas), TRAIL-R1 (CD120a), and TRAIL-R2 (DR5, KILLER, TRICK2). These receptors are activated by their corresponding death ligands. FADD (Fas-associated death domain protein, MORT1) and initiator procaspases are recruited by the receptor-ligand complex to form the DISC, death-inducing signalling complex. Procaspases are cleaved to become activated caspases and the intracellular cascade of apoptotic events is initiated (Schmitz et al., 2000; Igney and Krammer, 2002).

Unlike the extrinsic pathway, in the intrinsic path death stimuli are activated after intracellular damage is detected at various subcellular locations. In Figure 1.2, death stimuli lead to the activation of caspase 2, which cleaves the BH3 region-only protein Bid to its activated form, truncated Bid (tBid). The activities of other BH3-only, pro-

apoptotic proteins are regulated by transcriptional controls or post-translational modification. For example, in response to DNA damage, p53 mediates transcriptional activation of the BH3-only proteins NOXA and PUMA (Nakano and Vousden, 2001; Oda et al., 2000; Yu et al., 2001), whereas the presence or absence of growth factors dictate the phosphorylation required to inactivate the BH3-only protein Bad (Zha et al., 1996b; Datta et al., 1997). Activation of BH3-only proteins is the point of convergence of the two pathways and immediately precedes the activation of multi-BH region pro-apoptotic proteins Bax or Bak (Figure 1.2)(Wei et al., 2001).

Etoposide and serum starvation treatment, used to induce apoptosis in the experiments detailed in this project, both follow the intrinsic pathway of apoptotic induction. Etoposide is a commonly used chemotherapeutic drug which causes DNA damage by binding to topoisomerase II and stabilizing the intermediate product in which the enzyme remains bound to cleaved DNA (Hande, 1998). This persistent DNA strand break is detected by the cell and apoptosis is induced through the p53-mediated response discussed above (Ryan et al., 2001). The second method used to induce apoptosis was by incubating cells in little or no serum. This serum starvation deprives cells of sufficient amounts of growth factors that are necessary for survival. Growth factors, such as epidermal growth factor (EGF) and platelet-derived growth factor (PDGF) provide survival signals to cells through activation of phosphatidylinositol 3-kinase (PI3K), recruitment of additional kinases and activation by phosphorylation of Akt (PKB). Active Akt inhibits cell death through numerous mechanisms including phosphorylation of Bad, a pro-apoptotic Bcl-2 protein, thereby suppressing apoptosis and promoting cell survival

(Datta et al., 1999; Datta et al., 1997; Igney and Krammer, 2002). In the absence of serum, Akt is inactive, Bad is not phosphorylated, and is therefore active, able to bind anti-apoptotic proteins such as Bcl-xL to inhibit their pro-survival activity (Zha et al., 1996b; Datta et al., 1997). Additional survival promoting effects of Akt activation are the increased expression of inhibitor of apoptosis proteins (IAPs) by promoting NF-KB activity (LaCasse et al., 1998), blockage of activation of caspase 9 (Cardone et al., 1998) and sequestration of the forkhead family of transcription factors in the cytoplasm (Datta et al., 1999).

In both treatment methods used to induce apoptosis, deregulated expression of the protooncogene c-myc enhanced the cytotoxicity of treatment. The cell line used in these experiments, rat 1 myc ERTM fibroblasts, stably expresses myc-ERTM, a fusion protein of full length c-myc, a proto-oncogene which stimulates the cell cycle progression, with a mutant oestrogen receptor (Littlewood et al., 1995). In this configuration, c-myc is sequestered in this complex until cells are treated with 4-hydroxytamoxifen, a synthetic oestrogen analogue which binds to the receptor moiety thereby exposing a nuclear import signal. C-myc can then transactivate genes which sensitize and synchronize the cellular response to apoptotic stimuli (Evan et al., 1992; Littlewood et al., 1995; Soucie et al., 2001; Juin et al., 2002). Thus, all cells are treated with 100nm 4-hydroxytamoxifen as well as etoposide or low serum.

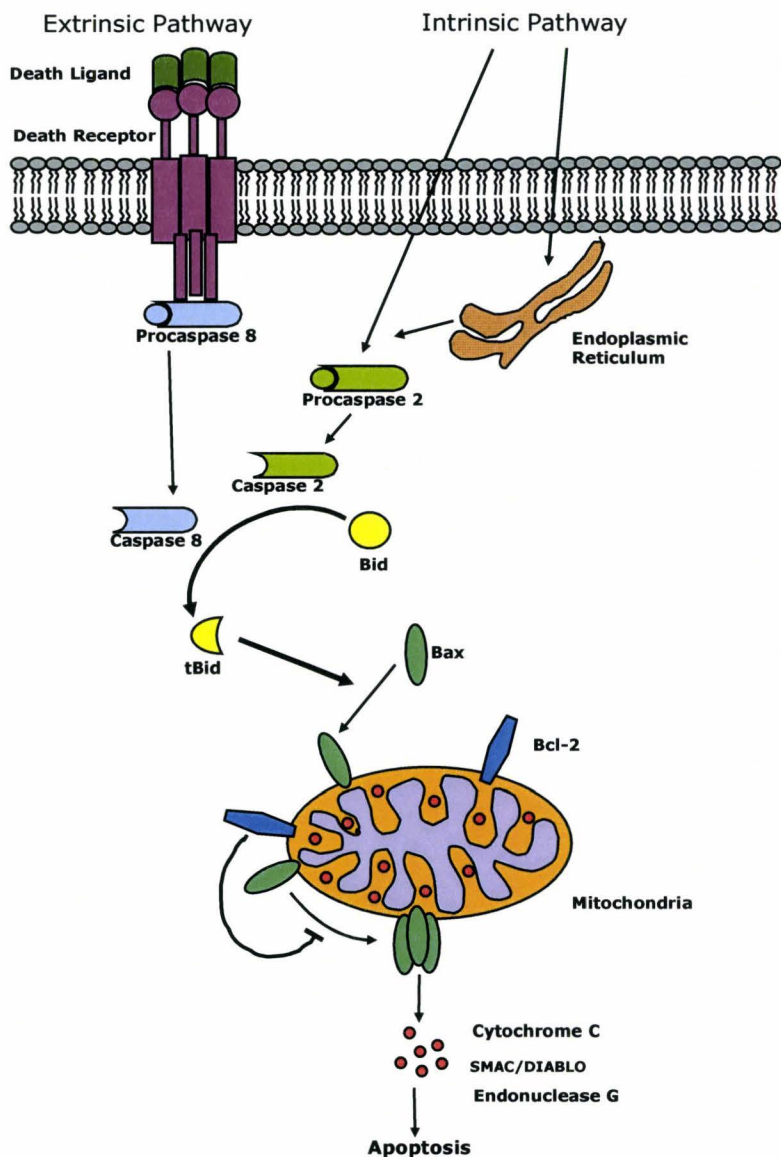


Figure 1.2 The Two Main Pathways of Apoptosis Initiation of apoptosis can occur via two paths. The extrinsic pathway is initiated through death receptors on the cell surface. When a death ligand interacts with a death receptor, the inactive pro-caspase 8 is cleaved to form activated caspases 8. In the intrinsic pathway, death signals are received directly at the organelle level, such as at the endoplasmic reticulum or mitochondria. The pathways converge at the mitochondria with the activation of BH3-region only pro-apoptotic proteins and continue in a common sequence of events. Activation of amplifier caspases, such as caspase 8 or caspase 2, facilitates further steps in apoptosis. At the

mitochondria, Bcl-2 proteins control the fate of the cell through an unknown mechanism. In this model, Bid is cleaved to yield the activated pro-apoptotic tBid, which then initiates translocation of pro-apoptotic Bax to the mitochondrial outer membrane. In a second regulated step, Bax then oligomerizes to form pores in the outer mitochondrial membrane thereby releasing proteins such as cytochrome c, SMAC/DIABLO and endonuclease G which go on to facilitate apoptosis (Igney and Krammer, 2002). Anti-apoptotic proteins such as Bcl-2 or Bcl-xL inhibit this process by preventing the translocation and/or oligomerization of Bax.

Caspases and Other Factors involved in Apoptosis

The two pathways of apoptotic initiation converge at the mitochondria. Here the apoptotic stimuli cause cells to undergo mitochondrial membrane permeabilization (MMP), the 'point of no return' for a cell (Kroemer and Reed, 2000). During MMP in mammals, many factors which act as apoptotic effectors are released from the mitochondria. One such protein is cytochrome c, which, when released from the mitochondrial inter-membrane space, binds to cytoplasmic Apaf-1 (apoptosis protease-activating factor-1). This results in the assembly of the apoptosome, a complex, made up of cytochrome c, Apaf-1, dATP/ATP and caspase 9 (Wang, 2001). In this complex, caspase 9 is activated to cleave other executioner caspases such as 3 and 7. This group of cysteine-specific aspartate-directed proteases are synthesized as pro-enzymes and activated at various stages of apoptosis. Active caspases go on to cleave specific cellular substrates, including other pro-caspases, activating downstream effectors of apoptosis, leading to cell death.

Historically, caspases were thought to be at the centre of control of apoptotic events, but recently new factors have been shown to play important roles in this process as well. In addition to Bcl-2 proteins, IAPs regulate apoptosis by binding and inhibiting caspases directly (Deveraux et al., 2001). AIF (apoptosis inducing factor), endonuclease G and SMAC/DIABLO (second mitochondria-derived activator of caspase/direct IAP binding protein with low pI) are three other mitochondrial proteins, in addition to cytochrome c, that are released into the cytoplasm during MMP in mammalian cells. AIF and endonuclease G both translocate to the nucleus and co-operate to cause the characteristic chromatin condensation and DNA fragmentation associated with apoptosis (Penninger and Kroemer, 2003). Although both proteins can work in a caspase independent manner (Li et al., 2001; Susin et al., 1999; Cande et al., 2002), at an intracellular level, it not known whether these factors work independently of, or in conjunction with, caspases. SMAC/DIABLO promotes downstream apoptotic events by binding to IAPs thereby antagonizing their ability to inhibit caspases (Du et al., 2000).

During apoptosis, certain caspases can activate members of the Bcl-2 family. Figure 1.2 illustrates a model of apoptosis in which the activation of caspase 8, in the death receptor-mediated pathway, or caspase 2 (Guo et al., 2002; Kuwana et al., 2002)), in the mitochondrial pathway, results in proteolytic activation of the BH3-region only, pro-apoptotic protein Bid (Figure 1.2). The cleavage of Bid generates t-Bid, which goes on to activate pro-apoptotic Bax facilitating the release of cytochrome c, endonuclease G and other proteins from the mitochondria. Other pro-apoptotic signals may activate distinct BH3-only molecules to effect the common pathway of Bax or Bak

oligomerization (Wei et al., 2000). This oligomerization is inhibited by the many different anti-apoptotic family members including Bcl-2 and Bcl-xL (Guo et al., 2002; Kuwana et al., 2002), preventing cytochrome c release and the progression of apoptosis (Cheng et al., 2001; Cory and Adams, 2002; Wei et al., 2000; Wei et al., 2001).

1.4 The Molecular Mechanism of Bcl-2

The Bcl-2 family of proteins are important regulators of apoptosis. Understanding how Bcl-2 proteins control this process is vitally important when designing new therapeutics for apoptosis resistant cells. Research into the membrane topology of Bcl-2 will help to determine the mechanism by which Bcl-2 inhibits apoptosis, and give further insight into potential cancer therapies based on exploitation of this protein.

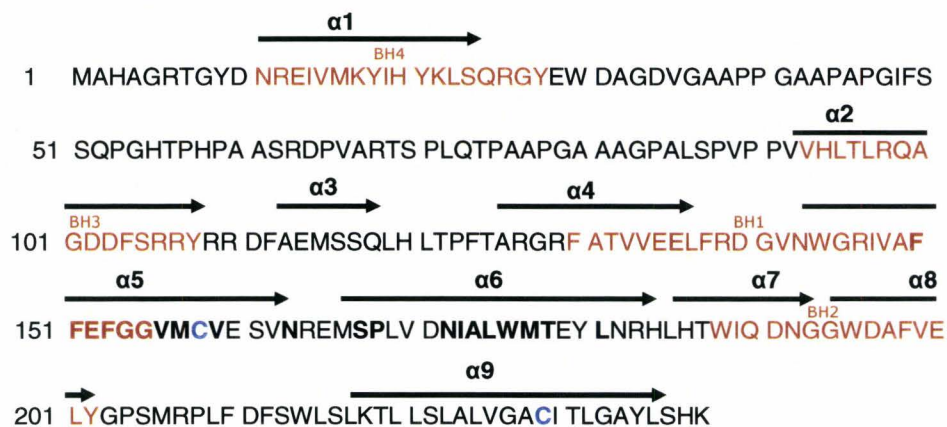
The mechanism of action of the anti-apoptotic proteins has not been elucidated, partly because studying membrane bound proteins is more difficult than cytoplasmic counterparts. Following the discovery that Bcl-2 prevents cytochrome c release from the mitochondria (Yang et al., 1997), many theories regarding the molecular mechanism have been proposed. Three main theories have emerged, each suggesting that Bcl-2 works at a different level in the apoptotic cascade. The first suggests Bcl-2 works upstream of Bax/Bak activation and MMP to physically prevent caspase activation (Adams and Cory, 2001; Marsden et al., 2002). The second proposes that Bcl-2 works at the level of the mitochondria or endoplasmic reticulum membrane, sequestering BH3-only proteins to inhibit their pro-apoptotic activity (Thomenius et al., 2003). Alternatively, the third suggests Bcl-2 at the mitochondrial membrane binds directly to multi-region pro-

apoptotic proteins such as Bax and Bak, thereby blocking the activation of these proteins and inhibiting mitochondrial membrane permeabilization (Cheng et al., 2001; Thomenius and Distelhorst, 2003).

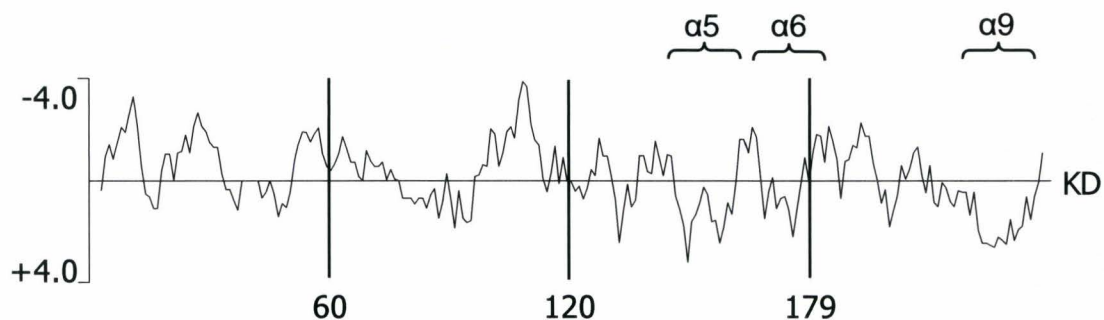
1.5 The Structure of Bcl-2

Wild type Bcl-2 contains nine α -helical domains (Figure 1.3a), including three with significant hydrophobic character (Figure 1.3b). The structure of Bcl-2 was determined using NMR spectroscopy. Due to the poor behaviour of Bcl-2 in solution, the structure was based on a chimeric protein of Bcl-2 and Bcl-xL (Petros et al., 2001). In the chimera, the unstructured loop of Bcl-2 was replaced with a shortened loop from Bcl-xL and the carboxyl-terminal tail was truncated resulting in a lower pI and increased solubility. In solution, the chimeric protein contained five amphipathic α -helices (grey) which surround and protect two hydrophobic helices (α 5 and α 6, red) (Figure 1.3c) by creating a hydrophobic pocket in the middle of the protein. It has been shown that the α 5 and α 6 helices are necessary for the anti-apoptotic function of Bcl-2 (Matsuyama et al., 1998).

a)



b)



c)

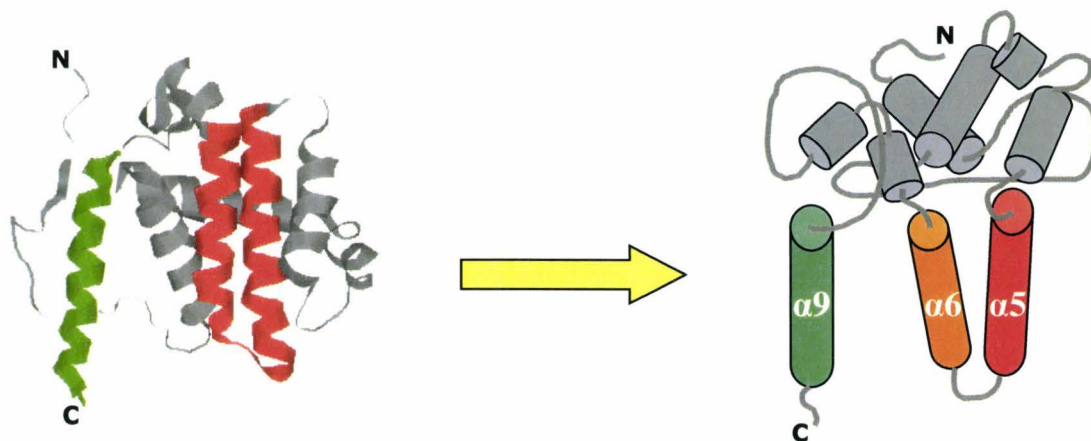


Figure 1.3 The Amino Acid Sequence, NMR Structure and Schematic

Representation of Bcl-2. a) The sequence of human Bcl-2, isoform 2. Blue residues indicate the locations of the endogenous cysteine residues, C158 and C229. Bold residues indicate the positions of introduced single cysteine residues in helices $\alpha 5$ and $\alpha 6$ in the context of a mutated protein in which the two endogenous cysteines have been changed (C158A, C229V); these cysteines were placed at positions 150-157, 159, 163, 167-168, 172-178, 181. The location of each helix, as determined by NMR, is shown with black arrows. The residues within each BH region are indicated in red. b) The hydrophobicity profile of Bcl-2 based on Kyte-Doolittle analysis (*Kyte and Doolittle, 1982*) made using Clone Manager 7.11 (Scientific and Educational Software, 2004).

Hydrophobic residues have positive scores; hydrophilic residues have negative. Each plotted point is the average value of 5 adjacent residues, plotted at the middle point. Amino acid numbers are indicated below the graph; Helices $\alpha 5$, $\alpha 6$ and $\alpha 9$ are indicated above. c) The NMR structure of Bcl-2 (Petros et al., 2001) represented by ribbons is shown, made using the modeling program RasMol. Five outer amphipathic helices, grey, surround two hydrophobic inner helices, $\alpha 5$ and $\alpha 6$, red. The amino (N) and truncated

carboxyl (C) termini are labelled. The third hydrophobic helix, $\alpha 9$, shown in green, was made separately and was added to represent a more complete protein. The cartoon on the left highlights the hydrophobic regions of Bcl-2, using red and green cylinders.

1.6 The Dynamic Membrane Topology of Bcl-2

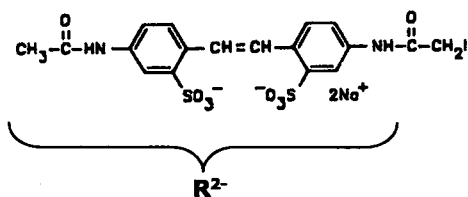
In microsomes and in healthy cells, Bcl-2 is found in a carboxyl-terminal tail-anchored topology (Janiak et al., 1994). The hydrophobic $\alpha 9$ helix is a carboxyl-terminal transmembrane (TM) domain which anchors Bcl-2 to the membrane, leaving the majority of the protein on the cytoplasmic face of the organelle (endoplasmic reticulum, mitochondria or nuclear envelope) (Wattenberg and Lithgow, 2001). Using the chemical label IASD (4-acetamido-4'-((iodoacetyl)amino)-stilbene-2,2'-disulfonic acid), a hydrophilic iodoacetamide that covalently modifies cysteine residues in aqueous environments, members of our lab have shown that Bcl-2 undergoes a conformational change after the induction of apoptosis (Kim et al., 2004) (Figure 1.4). The covalent modification of cysteine residues in aqueous environments adds two negative charges and causes a change in the electrophoretic mobility of the labelled protein in SDS-PAGE (Krishnasastri et al., 1994) and the isoelectric focusing gel system (Annis et al., 2005). Cysteines in hydrophobic transmembrane domains are protected from labelling. Bcl-2 has two endogenous cysteine residues, one in the carboxyl-terminal transmembrane domain (C229) and one in the $\alpha 5$ helix of the putative second transmembrane region (C158). In healthy cells, the C229 residue is protected by the membrane from being labelled in the

presence of 4M Urea and 16mM IASD. Urea is required in the labelling reactions in order to unfold the hydrophobic pocket of Bcl-2 and to disrupt any proteins bound to Bcl-2. However, in cells treated for 18 hours in 6 μ M etoposide or 48 hours in low serum conditions (0.03% serum), both C229 and C158 are protected from labelling. This protection from labelling can result if C158 were protected by the membrane, due the insertion of this portion of the α 5 helix into the membrane (Figure 1.4d). This is consistent with the multiple transmembrane region model of Bcl-2 suggested in the literature (Kim et al., 2004; Petros et al., 2004; Schendel et al., 1998).

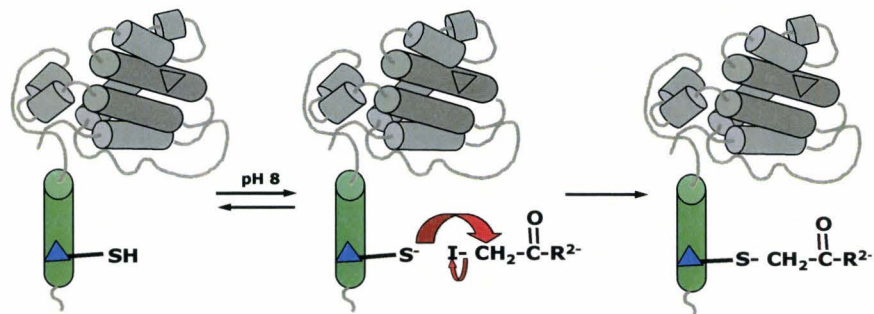
The pore forming, T region of diphtheria toxin has been shown to exist in two different topologies, depending on the nature of its environment. The structural similarity between this region of diphtheria toxin and Bcl-2 has led to the suggestion that Bcl-2 undergoes a similar change in topology triggered by environmental factors, going from a single membrane spanning domain protein to a polytopic membrane protein (Schendel et al., 1997; Matsuyama et al., 1998). Using cysteine scanning mutagenesis, Rosconi and London in 2002 showed that in the physiological pH of the cytoplasm, the α 8 and α 9 helices of diphtheria toxin's T region are shallowly inserted into the membrane, called the P conformation. In the low pH environment of the endosome, a conformational change occurs in which helices α 5- α 7 to insert into the membrane in addition to helices α 8 and α 9, called the TM conformation. This change in topology has been proposed to have functional significance, as it occurs before the subsequent protein-mediated translocation of the A chain of the toxin into the cytoplasm which facilitates cell death (Rosconi and London, 2002).

Many similarities exist between Bcl-2 and this region of diphtheria toxin. Bcl-2 also contains two hydrophobic regions. The first, in the $\alpha 9$ helix, is constitutively transmembrane in cells. The second, composed of helices $\alpha 5$ and $\alpha 6$, undergoes an environmentally sensitive conditional conformational change. The conditional transmembrane domains both contain a proline kink between the helices and a lower hydrophobic character than the domains which are always transmembrane. These structural similarities led to the suggestion that environmental factors could induce a similar change in topology of Bcl-2 from a carboxyl-terminal tail anchored protein to a polytopic membrane protein. In this new topology, shown in the top right panel of Figure 1.4d, helices $\alpha 5$, $\alpha 6$ and $\alpha 9$ are all inserted into the membrane (Schendel et al., 1998).

a)



b)



c)

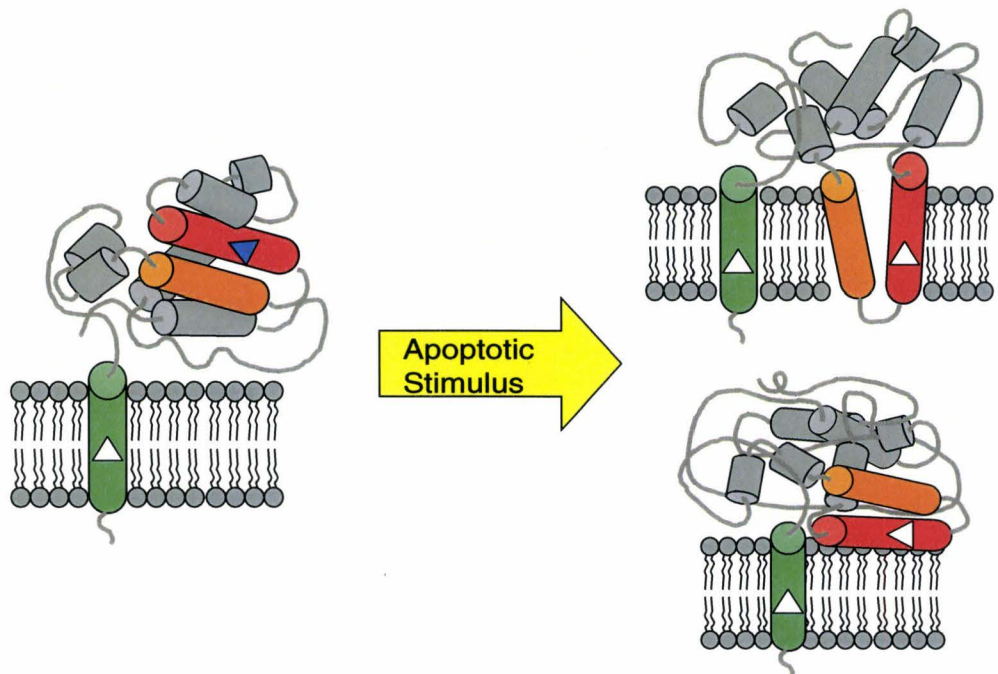


Figure 1.4 The Membrane Impermeant, Cysteine Specific Labelling Reagent, IASD, Used to Determine the Membrane Topology of Bcl-2 a) The structure of the R group of 4-acetamido-4'-((iodoacetyl)amino)-stilbene-2,2'-disulfonic acid (IASD). (Adapted from diagram by Dr M. Annis) b) A schematic representation of the covalent

modification of the thiol group on a cysteine residue by IASD. The addition of IASD to this residue adds two negative charges to the protein. c) The membrane topology of Bcl-2 in microsomes and healthy cells is shown on the left. Bcl-2, which has two endogenous cysteine residues (triangles in α helices 5, red, and 9, green), is anchored to the membrane via the carboxyl-terminal transmembrane domain (green). The majority of the protein, including C158 (blue triangle in the red cylinder) remains in the cytoplasm, while helix α 9, containing C229 (white triangle in the green cylinder), is located within the membrane. In this tail-anchored topology, Bcl-2 is anchored to the membrane by the carboxyl-terminal transmembrane domain (green). After the induction of apoptosis, shown on the right, Bcl-2 undergoes a conformational change which causes C158 (white triangle in the red cylinder) to become protected from IASD labelling. Two potential topologies are indicated to explain this change in labelling, but alternate conformations are possible.

Many possible topologies could result in the protection from IASD labelling of C158 during apoptosis. To determine the topology of Bcl-2 during apoptosis when it is functional, we took a systematic approach to determine the environment of each residue in the putative conditional transmembrane region to determine the most probable model. Using cysteine-scanning mutagenesis, a cysteine-specific, environmentally sensitive chemical labelling assay and an isoelectric focusing (IEF) gel system, I have shown that a discontinuous portion of helices α 5 and α 6 of Bcl-2 are protected from labelling after induction of apoptosis by etoposide or serum starvation in rat 1 myc ERTM fibroblasts.

The original IASD gel shift studies of labelled Bcl-2 by Dr P Kim in our lab were done using the Laemmli gel system. The band separation between labelled and unlabelled proteins was small, and results were sometimes difficult to interpret. For this project an alternate IEF gel system, originally optimised by Dr M Annis in our lab to separate IASD labelled Bax, was modified for Bcl-2. This system uses gels containing ampholytes that form a pH gradient and separate proteins based on their isoelectric point (pI). When a cysteine residue is modified by IASD, two negative charges are gained, the isoelectric point of the protein decreases and there is a large shift downward on the IEF gel. The labelling data were assembled in a topology map which is consistent with a model in which Bcl-2 changes from a carboxyl-terminal tail anchored, single membrane spanning protein in a “resting cell” to a polytopic protein, after the induction of apoptosis, in which helices $\alpha 5$ and $\alpha 6$ insert into and span the membrane.

CHAPTER 2: MATERIALS AND METHODS

2.1 General Materials

Chemical reagents used were purchased from Sigma-Aldrich Chemicals or Gibco-Life Science unless otherwise specified.

2.2 Antibodies

Three antibodies were used in the following experiments. To identify Bcl-2, a rabbit polyclonal antibody, STAN (at a concentration of 1:10,000) made in the Dr DW Andrews Lab (McMaster University) was used in combination with a goat anti-rabbit horseradish-peroxidase(HRP) secondary antibody(Jackson Immuno Research Laboratories Inc, 1:20,000). To identify the protein poly (ADP-ribose) polymerase, PARP, a mouse monoclonal primary antibody(C-2-10, Biomol, 1:20,000) was used with a donkey anti-mouse HRP secondary antibody (Jackson Immuno Research Laboratories Inc, 1:20,000). To confirm equivalent loading, actin levels were assessed by immunoblotting with a mouse monoclonal primary antibody (clone C4, ICN, 1:40,000) using a donkey anti-mouse HRP (Jackson Immuno Research Laboratories Inc., 1:20,000) as secondary antibody.

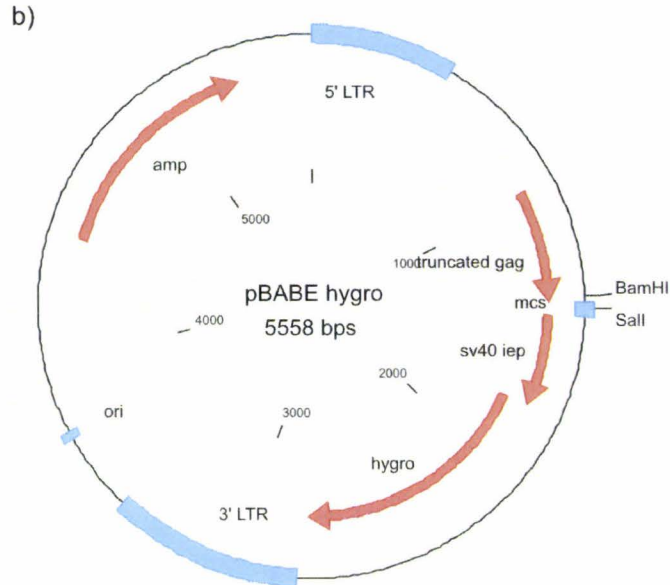
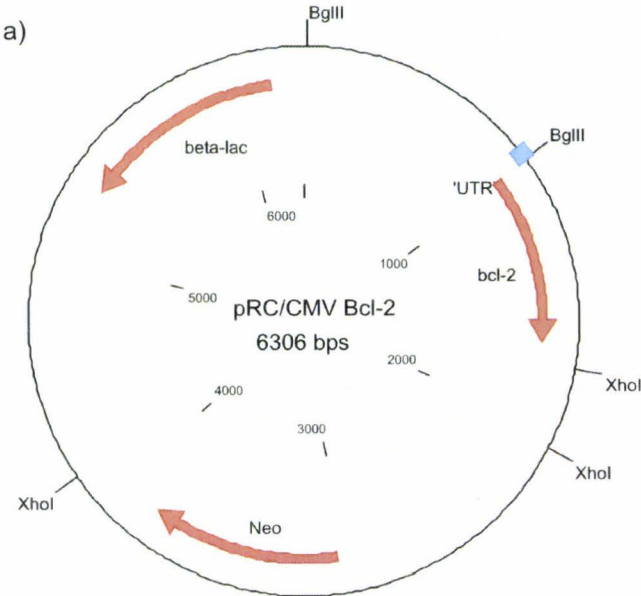
2.3 General Methods

2.3.1 Plasmids and proteins

Isolation, purification, digestion and mapping of DNA plasmids using restriction endonucleases were performed according to the protocols described in the DW Andrews laboratory manual (Andrews, 2005). Plasmids encoding Bcl-2 mutant proteins were constructed by Suzanne LaJolla in Dr J. Lin's lab (University of Oklahoma) using the full-length wild type Bcl-2 sequence in the backbone vector pSPUTK (DW Andrews laboratory plasmid #445). The cysteine-null Bcl-2 mutant (C0) and the first set of mutants assayed were generated by mutating both cysteine codons in the Bcl-2 coding region to valine and the methionine at position 157 to isoleucine (Bcl-2 M157I C158V C229V). Because this first set of mutants did not result in stable expression in rat 1 myc ERTM cells, a second set of mutant proteins were constructed in which the cysteine at position 158 was changed to alanine (designated Bcl-2, M157I C158A C229V). Alanine was used since it is a smaller, less hydrophobic amino acid than valine and may cause less disruption of folding. All mutagenesis was done using primers containing the desired mutations and using an overlapping PCR-based method (Ho et al., 1989; Zhang et al., 2004). The identity of the final plasmids was confirmed by DNA sequencing of the inserts. Bcl-2 single cysteine mutant proteins were generated by mutating the corresponding codon of the C0 mutant to a cysteine codon, and were designated by the location of the introduced cysteine. For example, G154C from the second set of proteins contained a cysteine at position 154 as well as the M157I, C158A and C229V mutations.

In order to make rat 1 myc ERTM cells which express the mutant Bcl-2 proteins, the DNA containing the coding region of each Bcl-2 mutant protein was shuttled from the pSPUTK plasmid to the vector pRC/CMV (Invitrogen, DW Andrews laboratory plasmid #655). This was done using the XbaI and HindIII sites which flank the Bcl-2 gene in the pSPUTK plasmid and are within the multiple cloning site of the pRC/CMV vector. All restriction enzymes were purchased from New England Biolabs (NEB) unless otherwise specified. Subsequently, the Bcl-2 coding regions were then subcloned into the retroviral vector pBABE hygro (DW Andrews laboratory plasmid #1748). The pRC/CMV Bcl-2 vector was digested with BglII and XhoI, yielding an 817 kDa fragment containing the Bcl-2 coding region (Figure 2.2a). The pBABE hygro vector was digested with BamHI and Sall, yielding a 5200 kDa fragment (Figure 2.2b). BglII, cuts the DNA at the 5' end of the Bcl-2 gene, leaving a 5' overhang which is compatible with the 5' overhang produced by BamHI. XhoI cuts at the 3' end of the Bcl-2 gene, leaving a 5' overhang, compatible with the 5' overhang produced by Sall. The DNA fragments were electrophoretically separated using 1.5% agarose gel and purified using the glass milk purification method detailed in the DW Andrews laboratory manual (Andrews, 2005). The ligation reactions were set up according to the DW Andrews laboratory manual and left at room temperature overnight. The following day the DNA was transformed using the 5 minute transformation methods detailed in the DW Andrews laboratory manual (Andrews, 2005) into DH5 α competent cells. The DW Andrews laboratory plasmid numbers for the pBABE hygro vectors containing the DNA coding sequences

corresponding to the mutant proteins used for further experiments in this project are listed in Table 1.



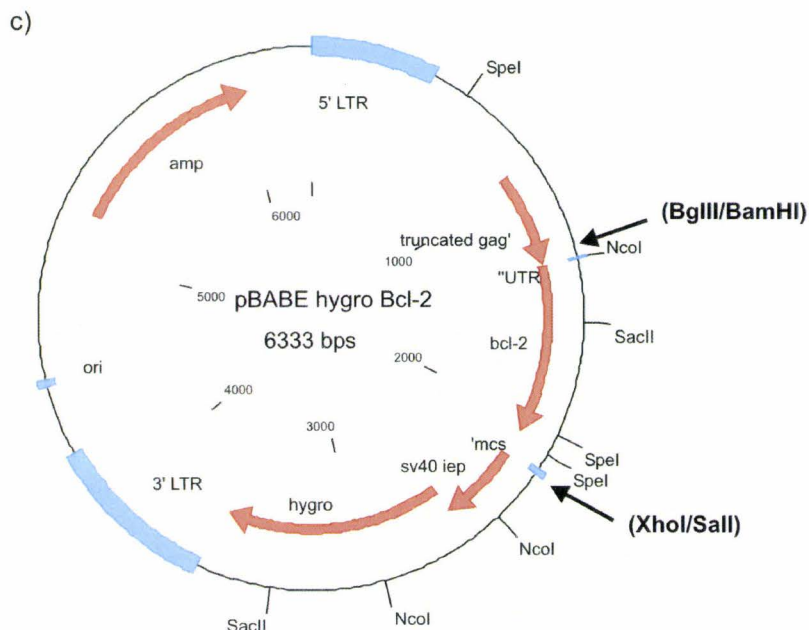


Figure 2.1 Plasmid maps of the pRC/CMV Bcl-2, pBABE hygro and pBABE hygro Bcl-2 vectors a) The pRC/CMV vector (Invitrogen, DW Andrews laboratory plasmid backbone #655) containing the Bcl-2 coding region (DW Andrews laboratory plasmid #656) was digested with BglII and XhoI, yielding an 817 bp fragment. b) The pBABE hygro retroviral vector (DW Andrews laboratory plasmid #1748) was digested using BamHI and SalI, yielding a 5200 bp fragment. BglII cuts the DNA at the 5' end of the Bcl-2 gene, leaving a 5' overhang compatible with the BamHI 5' overhang. XhoI cuts at the 3' end of the Bcl-2 gene, leaving a 5' overhang compatible with the 5' overhang produced by SalI. c) The resulting pBABE hygro Bcl-2 (DW Andrews laboratory plasmid #1749) vector has lost the BglII/BamHI and XhoI/SalI sites. To ensure the identity of the new plasmid, restriction digests were done with NcoI, SacII and SpeI and the region of the plasmid containing the insert was sequenced. All maps were made using Clone Manager 7.11 (Scientific and Educational Software, 2004).

Table 1 Mutant Bcl-2 proteins used for membrane topology analysis and their corresponding DW Andrews laboratory plasmid numbers

Protein	DWA lab Plasmid Number (Backbone 1748)
Wild Type	1749
F150 C	1896
F151 C	1897
E152 C	1898
F153 C	1899
G154 C	1900
G155 C	1901
V156 C	1902
M157 C	1903
V159 C	1904
N163 C	1905
S167 C	1906
P168 C	1907
N172 C	1908
I173 C	1909
A174C	1910
L175 C	1911
W176 C	1912
M177 C	1913
T178 C	1914
L181 C	1915
G154A/G155A	1940
V159D	1887

Note: All single cysteine mutants contain isoleucine at position M157, alanine at position C158 and valine at position C229. Additional mutants contain the wild type sequence with alanine at positions G154 and G155 (G154A/G155A) or aspartic acid at position V159 (V159D) and do not contain the isoleucine substitution at position M157.

Table 2 Mutant Bcl-2 C158V/C229V proteins obtained from Dr J Lin not used for membrane topology analysis and their corresponding DW Andrews laboratory plasmid numbers

Protein	DWA lab Plasmid Number		
	pSPUTK backbone (56)	pRC/CMV backbone (655)	pBABE Hygro backbone (1748)
Wild Type	445	656	1749
C0	1786	1639/1916*	1781
M16C	1787	1640	
K17C	1788	1641	
Y18C	1789	1642	
I19C	1790	1643	
W144C	1791	1644	
G145C	1792	1645	
R146C	1793	1646	1782
I147C	1794	1647	
F153 C	1795	1648	1783
G154 C	1796	1649	
G155 C	1797	1650	
V156 C	1798	1651/1917*	
M157 C	1799	1589/1918*	1784
C158	1800		
V159 C	1801	1591	
E160C	1802	1592	
V162C		1919*	
N163 C		1920*	
S167 C	1803	1921*	
P168 C	1804	1922*	
L169C	1805		
V170C	1806		
D171C	1807		
N172 C	1808		
I173 C	1809		
A174C	1810		
L175 C	1811	1653	

Table 2 - continued

Protein	DWA lab Plasmid Number		
	pSPUTK backbone (56)	pRC/CMV backbone (655)	pBABE Hygro backbone (1748)
W176 C	1812	1654	1785
M177 C	1813	1655	
T178 C	1814	1656	
E179C	1815		
Y180C	1816		
L181 C	1817		
N182C	1818		
R183C	1819		
H184C	1820		
L185C	1821		
T187C	1822		
W188C	1823		
I189C	1824		
Q190C	1825		
D191C	1826		
N192C	1827		
G227C	1828		
A228C	1829		
I230C	1830		

Note: All single cysteine mutants contain valine at positions C158 and C229, except those marked with an * which contain isoleucine at position M157, alanine at position C158 and valine at position C229.

Table 3 Mutant Bcl-2 proteins designed to disrupt dimerization obtained from Dr J Lin and their corresponding DW Andrews laboratory plasmid numbers

Protein	DWA lab Plasmid Number (Backbone 1748)
wt Q25R	1979
wt R107E	1881
wt Y108W	1882
wt S117W	1980
wt R139E	1883
wt D140W	1884
wt G141D	1885
wt N143R	1886
wt V159W	1888
wt E160R	1889

Note: All mutants contain the wild type sequence with only the specified mutations and do not contain the isoleucine substitution at position M157.

2.3.2 Transcription and Translation

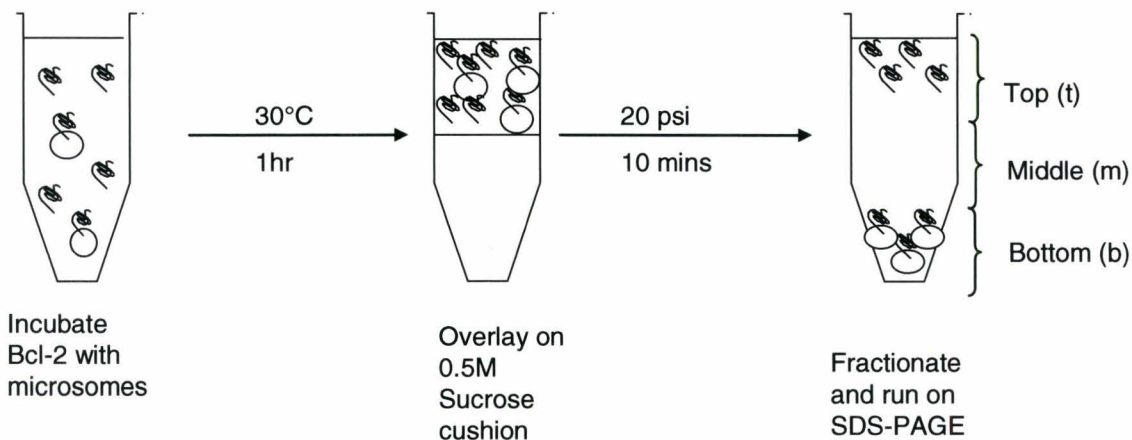
Transcription reactions were performed as described in (Gurevich et al., 1991) with SP6 polymerase (Fermentas) using the Bcl-2 single cysteine mutant coding sequences in the pSPUTK vector (T7 polymerase could not be used in these experiments because the Bcl-2 single cysteine mutants in the pSPUTK vectors contain promoter sequences for T7 polymerases both a 3' and a 5' of the coding region). Cell-free translation reactions were done using the rabbit reticulocyte lysate system (Jackson and Hunt, 1983) with [³⁵S]-methionine (NEN Perkin and Elmer) as described (Andrews et al., 1989).

2.3.3 Microsome targeting

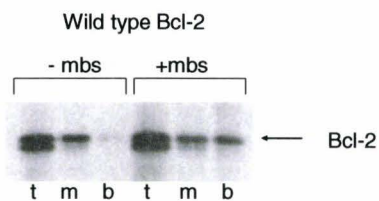
Crude canine pancreatic ER membranes (microsomes) obtained from Peter Kim, were used to test the targeting efficiency of the mutant proteins *in vitro*. Two separate translation reactions were incubated at 30°C for one hour in either the presence or absence of microsomes. These reactions were then layered over a sucrose cushion (50mM KCl, 2mM MgCl₂, 10mM Tris-HCl pH 7.5, 1mM DTT and 0.5M sucrose) in polyallomer tubes (Beckman). Microsomes were pelleted by centrifugation for 10 minutes at 20 psi (110000g) at 4°C in an airfuge. The supernatant was removed from the top in two equal fractions, top (t) and middle (m). The bottom (b) fraction was collected by solubilizing the pellet in 1% SDS and 0.1M Tris, pH 9.0 at 70°C for 10 minutes. TLB was added to each and equal volumes were separated by SDS-PAGE using the Tris Tricine buffer system described below. Gels were then dried for one hour at 80°C on a slab gel drier (BioRad), and visualized by exposing the gels to film overnight. Figure 2.2 shows autoradiographs of the targeting to microsomes of wild type Bcl-2, a single cysteine mutant containing only the endogenous cysteine in helix α 5 (Bcl-2 M57I/C229V, plasmid # 1800) and two single cysteine mutant proteins (Bcl-2 M157I/C158V/V159C/C229C , plasmid # 1801, and M157I/C158V/W176C/C229V, plasmid # 1812). The wild type protein targets to microsomes, as shown by the presence of a band in the bottom (b) fraction lane after incubation with microsomes, and the absence of a band when incubated without microsomes. However, none of the Bcl-2 mutants with valine at positions C158 and C229 tested (Figure 2.2c) targeted to

microsomes with the same efficiency as the wild type protein and thus were not used for further experiments.

a)



b)



c)

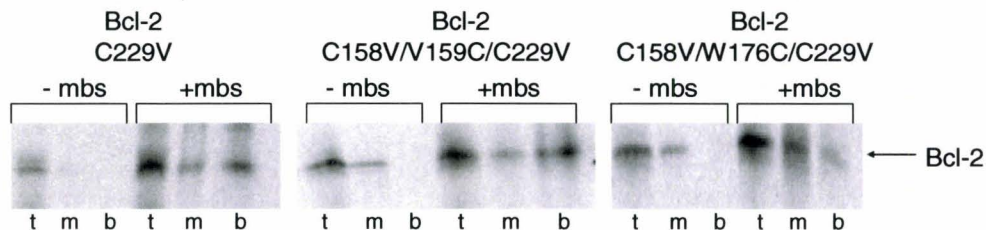


Figure 2.2 Microsome targeting assay using [³⁵S]-Methionine labelled wild type Bcl-2 and single cysteine mutants a) Proteins synthesized *in vitro* were incubated with crude ER microsomes, overlaid on a 0.5M sucrose cushion, and centrifuged for 10 minutes at 20 psi (110000 x g) at 4°C in an airfuge. The supernatant was fractionated into top (t) and middle (m) fractions. The pellet (bottom, b) was resuspended in 1% SDS buffer. The autoradiographs show the location of the [³⁵S] methionine labelled wild type Bcl-2 b) and the Bcl-2 mutants C229V, C158V/V159C/C229V and C158V/W176C/C229V after incubation with (+mbs) and without (-mbs) microsomes c). Proteins targeted to microsomes present in the bottom fraction. The absence of a protein band in the bottom fraction of a -mbs sample, and the presence of a band in the bottom of the +mbs sample, indicates that proteins have successfully bound to the microsomes.

2.3.4 Tissue Cell Culture

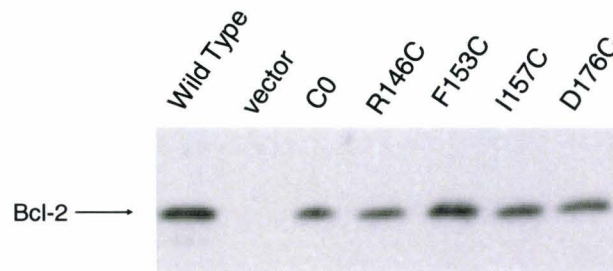
Rat 1 myc ERTM fibroblasts were cultured in α -minimal essential medium (α MEM, Invitrogen) supplemented with 10% fetal bovine serum (FBS, HyClone). Phoenix cells were grown in Dulbecco's Modified Eagle Medium (DMEM, Invitrogen) supplemented with 10 % FBS (HyClone).

2.3.5 Transfection and Retroviral Infection of Rat 1 myc ERTM fibroblasts

Bcl-2 mutant constructs in the pRC/CMV vector were transfected into rat 1 myc ERTM cells using ExGen500 (Fermentas) according to the manufacturer's protocol. ExGen500 is made up of linear polyethylenimine (PEI) molecules. These highly branched aliphatic polyamine molecules form complexes with and condense DNA. These

complexes settle on the cell surface and are taken up by endocytosis. Every third atom of PEI is an amino nitrogen which can be protonated. This characteristic allows it to extract protons from its environment facilitating endosome buffering and protection from lysosomal degradation while translocating DNA to the nucleus (Godbey et al., 1999). Retroviral infections were done using the viral packaging cell line, Phoenix-Eco. Bcl-2 mutant constructs in the pBABE hygro retroviral vector were transfected into Phoenix-Eco cells using ExGen 500 where it is replicated, packaged in virus and released from the cell. Ten μg of DNA and 6 equivalents of ExGen transfection reagent in 0.5 ml of 150mM NaCl were added to 4.5ml DMEM (with 10%FBS) on Phoenix-Eco cells (50% confluent) in 50mm flasks (Corning) and left overnight at 37°C. The following day media was changed and left overnight at 32°C. Viral supernatants were then collected and filtered through 0.2 μm filter. Parental cells (60% confluent) were incubated in 100mm flasks (Corning) at 32°C overnight, with 5ml of viral supernatant, 3 ml of fresh media (α MEM with 10% FBS) and 8 μl of Polybrene (Sigma, 0.8mg/ml in 150mM NaCl). Cells were passaged in selection media (α -MEM, 10% FBS, 180 $\mu\text{g/ml}$ hygromycin) for one week, at which time uninfected cells in control dishes were all dead.

a)



b)

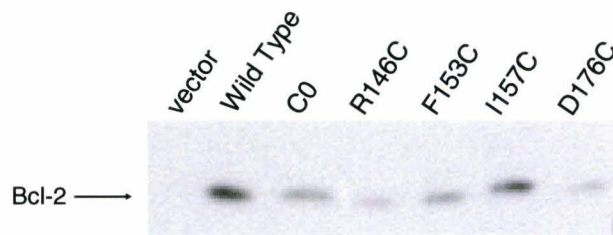


Figure 2.3 Expression of Bcl-2 C158V/C229V mutant proteins in rat 1 myc ERTM fibroblasts Rat 1 myc ERTM fibroblasts were infected with retrovirus to express either wild type Bcl-2 or a single cysteine mutant, as indicated. Cells were harvested in 1% SDS lysis buffer, and 8 μ l of total protein were run in each lane. The cells were lysed at one passage, a), and three passages, b), after infection. Subsequent experiments showed little to no expression after this passage.

2.3.6 Cell Death Assays

Rat 1 myc ERTM cells (60% confluent) expressing wild type or a single cysteine mutant of Bcl-2 were treated with 4-hydroxy tamoxifen (Sigma, 100nM) and either etoposide (6 μ M, for 12 and 18 hours) or low serum conditions (0.03% FBS, for 24 and 48 hours) to induce apoptosis.

2.3.7 Preparation of Whole Cell Lysates

One 100 mm cell culture dish (Sarstedt) of rat 1 myc ERTM cells was used for each treatment time point. Cells were harvested using a rubber policeman, transferred into 15ml Falcon tubes and pelleted by centrifugation in a clinical centrifuge at 1000g for 3 minutes at 4°C. Pellets were resuspended and washed twice in cold phosphate buffered saline (PBS). 200 μ l of hot SDS lysis buffer (10mM Tris-HCl pH7.5, 10mM NaCl, 1% SDS, 95°C) was then added to the final pellet and passed through a 26-gauge needle eight times. Samples were centrifuged in the microcentrifuge (Eppendorf) at 10,000x g for 10 minutes to remove any undissolved cell debris from the supernatant. 5 μ l of sample was added to 45 μ l of water and this sample was used for protein quantification. Tricine loading buffer (TLB, 4% SDS, 0.1M Tris-HCl pH 8.9, 2mM EDTA, 0.1% bromophenol blue, 20% glycerol, 0.25M DTT) was added in a 1:1 ratio to the remainder of the sample, followed by snap freezing in liquid nitrogen and storage at -20°C.

2.3.8 Preparation of Subcellular fractions from Cell Extracts by Nitrogen Cavitation

Ten 100 mm culture dishes (Sarstedt) of rat 1 myc ERTM cultured cells were used for each treatment condition. The cells were harvested using a rubber policeman, transferred into 50 ml Falcon tubes and pelleted by centrifugation in a clinical centrifuge at 1000g for 3 minutes at 4°C. The pellet was washed twice with cold cell buffer (250 mM Sucrose, 20 mM HEPES pH 7.5, 2 mM MgCl₂, 1 mM NaEDTA, 1 mM DTT and protease inhibitors (0.2 µg/mL of chymostatin, antipain, leupeptin, pepstatin and 0.4 µg/mL of aprotinin)). The final pellet was resuspended in 2ml of cell buffer. This suspension was held at 150 psi for 15 minutes on ice in a 45 ml Nitrogen Bomb (Parr Instruments) and cells were disrupted by releasing the pressure. The nuclei, cell debris and unbroken cells in the expelled lysate were removed by microcentrifugation (Eppendorf) at 500x g for 3 minutes. The heavy membrane fraction, enriched with mitochondria and endoplasmic reticulum, was separated from the resulting supernatant by centrifugation at 100,000 x g for 1 hour at 4°C in an ultracentrifuge (Beckman) using a TLA120.2 rotor (Annis et al., 2001). The pellet was subsequently resuspended in cell buffer. 5µl of sample was removed and added to 45µl of water to use for protein quantification and the remainder was snap frozen in liquid nitrogen and stored at -80°C.

2.3.9 Protein Sample Quantification

The BCA assay (Pierce) was used according to the manufacturer's protocol to quantify the total protein in the SDS lysates (8µg of total protein was run in each lane on SDS PAGE). The Bradford assay (Bio-Rad) was used according to the manufacturers

protocol to quantify total protein in the heavy membrane fraction of samples prepared by Nitrogen cavitation (75 μ g of total protein was used for each IASD labelling experiment). A new standard curve of protein concentrations was constructed using BSA for each experiment; sample concentrations were determined according to this curve.

2.3.10 Protein Electrophoresis

Three different polyacrylamide-gel electrophoresis (PAGE) systems were used for protein separation. To separate proteins in whole cell SDS lysates, samples were analyzed by SDS-PAGE using 10% Tricine gels (Schagger and von Jagow, 1987). The second was the Laemmli gel system (Laemmli, 1970), used in initial experiments to separate IASD labelled Bcl-2 and Bcl-xL from unlabelled protein. These 16% acrylamide gels were 12 cm long, and were run for 15 hours at 10mA to resolve the small shift of IASD labelled Bcl-2. However, better resolution of IASD labelling was achieved with the third type of gel system used, the isoelectric focusing (IEF) gel system. The IEF system uses gels containing ampholytes that form a pH gradient to separate proteins based on their isoelectric point (pI). When a cysteine residue is modified by IASD, two negative charges are gained, the isoelectric point of the protein decreases and there is a shift downward on the IEF gel. Samples were run on gels with a pH 5-8 ampholyte range (1.5% 5-8 ampholytes (Bio-Rad), 0.5 % 3-10 ampholytes (Bio-Rad), 5% acrylamide (40%T/3%C BioShop), 4M Urea (BioShop), 4% IGEPAL-630 (Sigma, also referred to as NP-40) and 2% CHAPS (BioShop)). Gels were pre-run at 100V for at least 30 minutes before samples were added. Buffers were exchanged, samples were loaded and the gels were run

at 100V, 250V, 500V and 700V for 1 hour each followed by 900V for 15 minutes, or until the dye front reached the level of the anode. Gels in which the dye front ran below the level of the anode resulted in a decrease in the sharpness of band focusing.

2.3.11 Immunoblotting

Proteins from all gel systems used were transferred to PVDF membranes (Pall Life Sciences). The Tricine and Laemmli gels were soaked for 10 minutes in Transfer buffer (3mM Tris, 24mM glycine, 20% methanol). PVDF membranes were wet with methanol followed by transfer buffer. Three pieces of blotting paper (Whatman), wet with transfer buffer, were placed beneath the PVDF membrane on the Hoefer semi-dry transfer apparatus (Pharmacia Biotech). Each gel was placed on top of the membrane, under two more pieces of blotting paper wet with transfer buffer. Air bubbles between the layers were rolled out and proteins were transferred for 1 hour at 50mA per gel, with cooling. To transfer proteins from the IEF gels, two transfer buffers were used. Gels were soaked in 1% acetic acid then 1% acetic acid with 4% SDS for 5 minutes each, at which point horizontal white bands are seen across the gels. The blotting papers beneath the gel and the PVDF membrane were saturated with 1% acetic acid and the top blotting papers were saturated in 1% acetic acid with 4% SDS.

After transfer, all membranes were blocked in Blocking Buffer (10mM K_2PO_4 pH 7.4, 140mM NaCl, 0.02% NaN_3 , 5g/L powdered milk) at room temperature for 30 minutes and then washed in TBS-T (10mM Tris-HCl pH 7.4, 500mM NaCl, 0.2% Tween 20) and incubated overnight at 4°C in primary antibody diluted in TBS-T with 1% BSA.

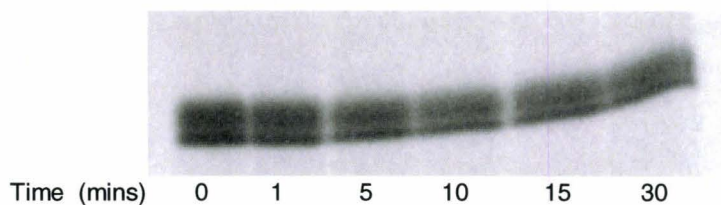
Membranes were washed for 10 minutes three times in TBS-T and incubated with HRP-conjugated secondary antibody for 2 hours at room temperature in TBS-T with 1% BSA. Membranes were then washed for 10 minutes three times in TBS-T, exposed to film and developed using the Enhanced Chemiluminescence (ECL) method (Perkin Elmer).

2.3.12 IASD labelling reactions

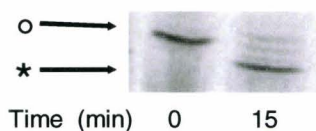
The chemical labelling gel shift assay used as described by Kim et al 2004 (Kim et al., 2004) was adapted from that used in Krishnasastri et al 1994 (Krishnasastri et al., 1994). The environment of cysteine residues in each Bcl-2 protein was determined by incubation of the membrane fraction of cell lysates with IASD (Molecular Probes). Initial IASD labelling experiments in our lab were done using *in vitro* synthesized, [³⁵S]-methionine (NEN Perkin and Elmer) labelled Bcl-2 and the Laemmli gel system. Experiments done by Peter Kim using single cysteine mutants showed that in the absence of membranes, the endogenous C229 (in helix α 9) is labelled by IASD before C158 (in helix α 5), because C158 is situated in a hydrophobic pocket that must be unfolded (by Urea) before it can be modified by IASD. Therefore all labelling reactions included 4M Urea. Conversely, when Bcl-2 is first targeted to microsomes and then labelled with IASD it is C158 which labels first. This is because C229 is located in the carboxyl-terminal transmembrane domain which inserts into the bilayer, protecting this residue from IASD modification. The band separation of the gel shift associated with IASD labelled Bcl-2 is small when using the Laemmli system. The gel shift associated with IASD labelled Bcl-xL could not be resolved using the Laemmli system because no

difference was detected between the labelled and unlabelled lanes (Figure 2.5, a). The IEF system was able to resolve this shift (Figure 2.5, b and c). Labelling was done in the targeting buffer (50mM KCl, 2mM MgCl₂, 10mM Tris-HCl pH 7.5, 1mM DTT) with 4 M Urea at pH 8, with a total volume of 60 μ l. Twenty μ l was removed at time 0 to use as an unlabelled control (T=0). Twenty μ l was incubated in 10mM IASD for 10 minutes (T=10) and 20 μ l was incubated in 10mM IASD with 2% Triton X-100 for 10 minutes (Det). Labelling reactions were quenched with 100mM of DTT (20x excess). Samples were sonicated for 15 minutes at 4°C, diluted 1:1 with TLB and run at 10mA for 15 hours on Laemmli gels. Figure 2.4 shows autoradiographs of IASD labelled, [³⁵S]-methionine labelled Bcl-xL (a, b) as well as a western blot of IASD labelled, affinity-purified Bcl-xL(c) (protein obtained from Jeremy Yethon). The gel shift associated with IASD labelled Bcl-xL using the Laemmli system was blurred and the unlabelled protein was indistinguishable from the labelled protein (Figure 2.4a). However, using the IEF gel system, using a pH 4-6 ampholyte range, the shift was clearly resolved (Figure 2.4b). Labelling of the cysteine in Bcl-xL is shown by a shift down in the location of the Bcl-xL band because IASD modification caused the pI of Bcl-xL to decrease and thus shift down to a lower pH in the gel.

a)



b)



c)

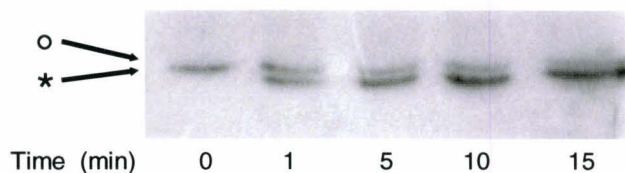


Figure 2.4: IASD labelling of Bcl-xL. (a) An autoradiograph of IASD labelled wild-type Bcl-xL, synthesized using the rabbit reticulocyte lysate method (Falcone and Andrews, 1991). The [³⁵S]-methionine-labelled Bcl-xL was incubated in 10mM IASD and 4M Urea for 0, 1, 5, 10, 15 and 30 minutes and resolved using the Laemmli gel method (Laemmli, 1970). No band shift was shown. (b) An autoradiograph showing the downward band shift of IASD labelled Bcl-xL in an IEF gel, by 15 minutes of labelling. In c) affinity-purified protein Bcl-xL is almost completely labelled after 15 minutes of incubation in IASD resolved using the IEF gel system. IASD modification causes a decrease in the pI of Bcl-xL, causing a shift down toward the lower pH area of the IEF gel. (* denotes one labelled cysteine and ° denotes no labelled cysteines).

IASD labelling reactions with the isolated heavy membrane fraction from cells over-expressing Bcl-2 were done using 75 μ g of total protein in 30 μ l of cell buffer (250 mM Sucrose, 20 mM HEPES pH 7.5, 2 mM MgCl₂, 1 mM NaEDTA, 1 mM DTT and protease inhibitors). An equal volume of Urea buffer (UB, cell buffer pH9.5 with 8M Urea) was added to bring the final concentration of Urea to 4M with a pH of 8. The reaction was mixed gently and twenty μ l was removed at time 0 to use as an unlabelled control (T=0). Twenty μ l was incubated in 16mM IASD for 10 minutes (T=10) and the remaining 20 μ l was incubated in 16mM IASD with detergent(s) for 10 minutes (Det). In experiments where the Laemmli system was used, the detergent used in the Det sample was Triton X-100 (2%). When the IEF gel system was used the detergents used were Triton X-100 (2%), IGEPAL (4%) and CHAPS (2%). All reactions were quenched with 160mM of DTT (20x excess). The same detergent(s) in the detergent control were then added to each of the other two samples (T=0 and T=10) before the samples were sonicated for 15 minutes at 4°C. For the Laemmli system, TLB was added to each sample (1:1 ratio). In the IEF system 3 μ l of IEF loading buffer (50% glycerol and trace bromophenol blue) was used. In the two outermost lanes in both gel systems loading buffer alone was added. This ensured the horizontal running of the dye front, as running empty lanes at the gel margins caused the inner lanes to run faster and the dye front to appear curved.

2.3.13 Optimization of the Resolution of the Band Shift Associated with IASD labelled Bcl-2 using an Isoelectric Focusing Gel System

The resolution of IASD labelled Bcl-2 using the Laemmli gel system showed very small band shifts that were inconsistent and hard to interpret. An alternative gel system was investigated to improve the resolution of IASD labelled Bcl-2. The IEF system had been optimized by Dr Matt Annis in our lab for resolution of IASD labelled BAX (Annis et al., 2005). The initial experiments using this system to resolve Bcl-2 were very hard to interpret, and optimization of this system for Bcl-2 was required. Three major problems were identified and the appropriate changes made:

1. Bcl-2 bands appeared smeared

- Gels were run at higher voltages, for shorter times to sharpen focusing.
 - Initial resolution was done at 100V, 250V and 500V for one hour each
 - The resolution was found to be optimal when run at 100V, 250V, 500V and 700V for 1 hour each and 900V for 15 minutes
- Less total protein was used in the labelling reaction
 - Initial experiments were done with over 100µg of total protein (Figure 2.5 a)
 - 75µg of total protein was found to show the clearest labelling results (Figure 2.5 e)

- #### **2. A portion of sample in each lane appeared not to enter the gel, as shown by protein bands on western blots in the base of the wells**

- Initial samples contained only the detergents IGEPAL (4%) and CHAPS (2%) (Figure 2.5 a)
- Triton X-100 (2%) was added to all samples at the same concentration as the detergent lane, because the detergent lane consistently had better sample entry than the other two lanes
 - With final detergent concentrations of Triton X-100 (2%), IGEPAL (4%) and CHAPS (2%), the amount of protein entering the gels increased. (Figure 2.5 c-e)
- Sonication was extended from 5 minute to 15 minutes to solubilize more protein and mitochondrial DNA
 - Longer sonication increased the amount of protein entering the gel (Figure 2.5 d, e)
 - Optimal sample entry and band resolution occurred with the detergent combination IGEPAL (4%), CHAPS (2%) and Triton X-100 (2%) and 15 minutes of sonication, (Figure 2.5 e)
- Addition of DNase and heating samples at 65°C for five minutes were tested but failed to improve results (data not shown)

3: Membranes were not intact during labelling, as shown by the presence of a band indicating that residue C229 was being labelled in the reaction

- Membrane isolation by centrifugation after labelling was attempted to isolate intact membranes

- Centrifugation caused too much protein loss, and was therefore not adopted in the final procedure (Figure 2.5 b)
- Frozen samples were thawed quickly at 37°C for 5 seconds, instead of thawing on ice (Figure 2.4 e)
- Handling of samples was kept to a minimum, and labelling was done immediately upon thawing
- Overall reaction time was decreased from 15 minutes of labelling to 10 minutes of labelling
 - The presence of the band indicating labelling of C229 decreased, and significantly less degradation appeared after making these changes (Figure 2.5 a vs., e)

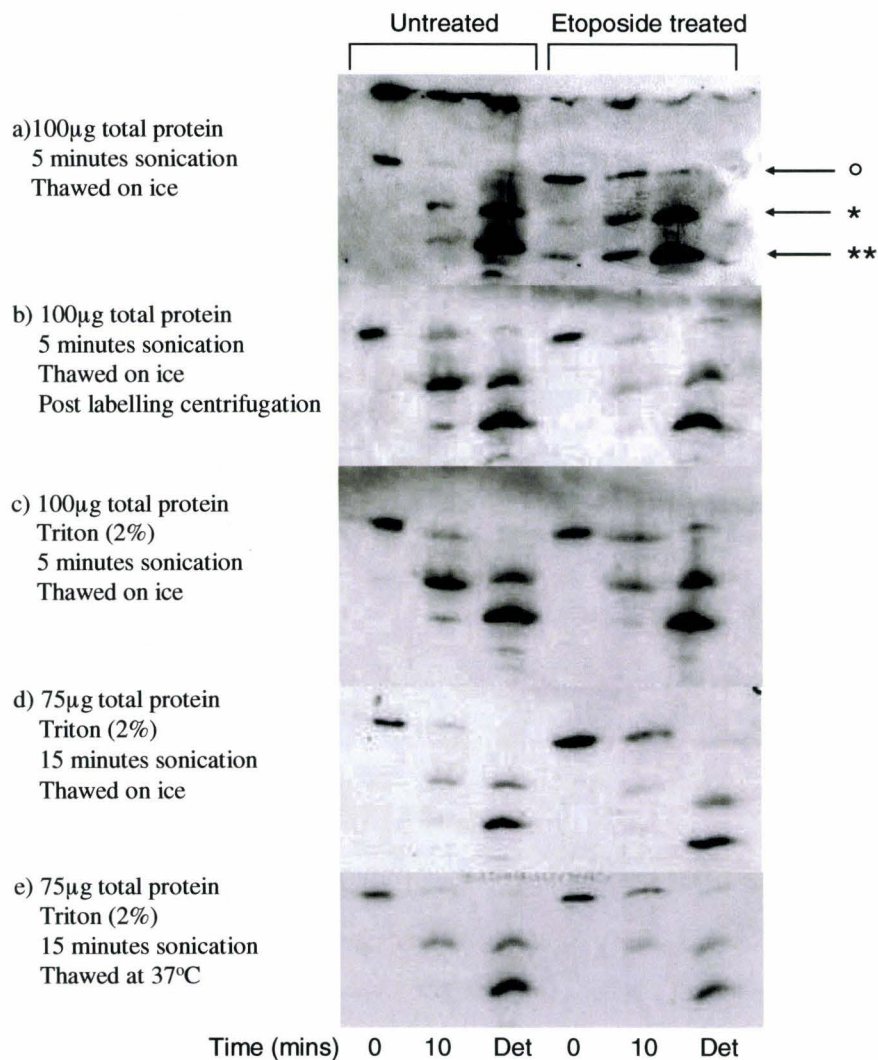


Figure 2.5 Optimization of the isoelectric focusing gel system to resolve the band shift associated with IASD labelled Bcl-2 Examples of western blots during optimization of the gel shift assay using IASD labelled wild type Bcl-2 are shown. Cells were lysed by nitrogen cavitation, nuclei were removed and the membrane fraction was isolated by ultracentrifugation. Labelling reactions were done in cell buffer with 4M Urea at pH 8. The unlabelled (T=0) lane indicates samples incubated without IASD. In the labelled lane (T=10) and the Detergent (Det, Triton X-100 (2%)) lane samples were

incubated in 16 mM IASD for 10 minutes. DTT (160mM final) was added to each sample to stop labelling. Proteins were transferred to PVDF membranes and immunoblotted for Bcl-2. (**denotes two labelled cysteine residues, * denotes one labelled cysteine and ° denotes no labelled cysteines). Many optimization steps were taken to improve the blurry resolution of bands shown in a), such as post-labelling membrane isolation by centrifugation (b), addition of Triton X-100 (c-e), fast thawing at 37°C (e) and extended sonication (d,e). The western blot in e) represents results obtained using the optimal conditions.

2.3.14 Quantification of Western Blots

Western blot films were scanned and band intensities were quantified using Image Quant Software, which measures the volume intensity of each band in a designated area. Boxes of equal size were constructed to surround each band in one lane. Background readings were calculated using the average per pixel intensity of the area covered by the lines of the box. This method of background correction provided the most reliable results when compared to using the median value or manual correction, although there was little difference between the methods (data not shown). The background value was automatically subtracted from the volume of intensity within each box and the net intensity was reported. For PARP cleavage experiments further calculations were done to determine the percent of PARP cleavage at each time point. The net intensity of the cleavage product band was divided by the sum of the net cleaved and uncleaved band intensities in each lane. This value was multiplied by 100 to get a percentage. Analysis of

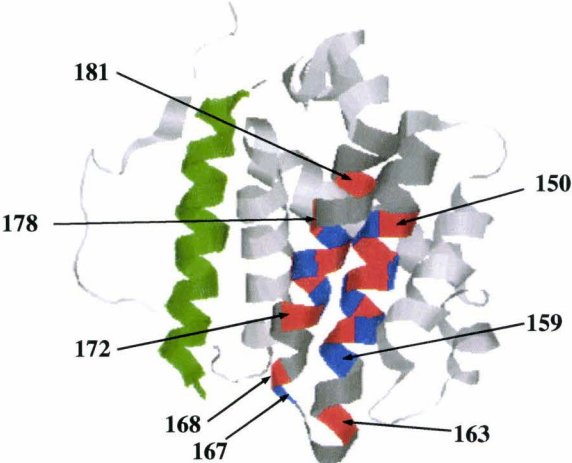
variance (ANOVA) tests were done using the data from each time point; means, standard deviations and 95% confidence interval (CI) tables were created to compare the results from each protein to the wild type. For IASD labelling experiments further calculations were done to determine the percent of unlabelled protein after ten minutes of IASD labelling. The net intensity of the unlabelled band was divided by the sum of the net labelled and unlabelled band intensities in the ten minute lane. This value was multiplied by 100 to get a percentage. ANOVA tests were done using the data from each experiment. Means, standard deviations and 95% confidence interval (CI) tables were created to compare the results from each protein to the wild type. Data from at least three replicate labelling experiments were collected and used for the statistical analysis.

CHAPTER 3: RESULTS

3.1 Expression of Bcl-2 mutants in rat 1 myc ERTM fibroblasts after retroviral infection

To investigate the membrane topology of Bcl-2 before and during apoptosis, two different series of Bcl-2 mutant proteins were used. The first set of twenty mutants contained single cysteine residues at various positions in the $\alpha 5$ and $\alpha 6$ helices of Bcl-2 in which the two endogenous cysteines had been changed to alanine and valine (Bcl-2 M157I/C158A/C229V, see Figure 3.1). The second set of twelve mutants consisted of a series of single or double point mutations and contained the endogenous cysteine residues. These mutations were designed by Dr J Lin to disrupt Bcl-2 homodimerization as predicted by molecular modelling programs. Based on functional analysis demonstrating an altered potency at inhibiting apoptosis, two mutants were chosen from this group for further study, Bcl-2 V159D and Bcl-2 G154A/G155A (referred to as V159D, G154A/G155A).

a)



b)

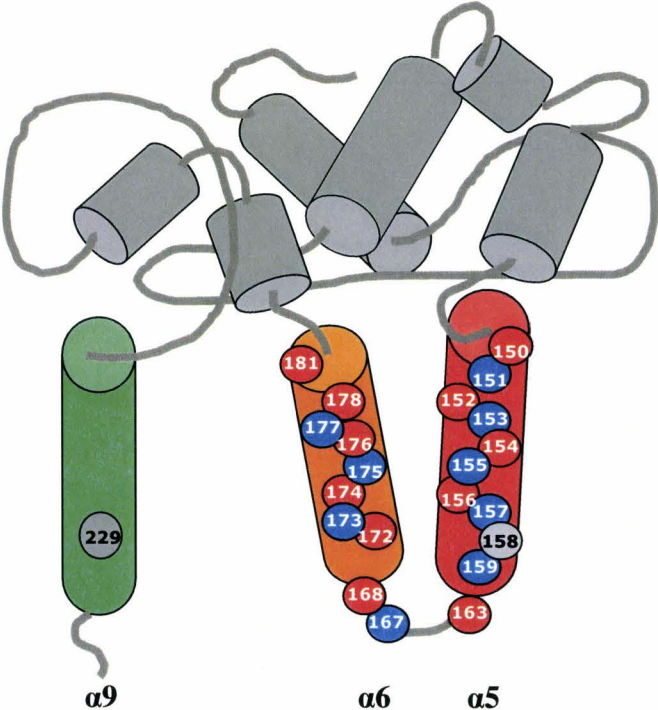


Figure 3.1 Position of the Bcl-2 single cysteine mutants DNA sequences coding single cysteine mutants of Bcl-2 M157I/C158A/C229V were constructed in the laboratory of our collaborator Dr J. Lin and subcloned into the pBABE hygro retroviral vectors by members of both the Lin and Andrews labs. a) The positions of individual cysteine residues are indicated by alternating red and blue circles at positions 150-157, 159, 163, 167-168, 172-178, 181 on the modified NMR structure of Bcl-2 derived from (Petros et al., 2001). Helix α_9 , not included in the NMR structure, has been added in green in a position to simplify visualization. b) The single cysteine residue positions shown on the schematic cylinder diagram of Bcl-2. Residues are indicated by alternating red and blue circles on helix α_5 (red cylinder) and helix α_6 (orange cylinder). The grey circles indicate the locations of the endogenous cysteine residues, C158 and C229, which were changed to alanine and valine, respectively, in the mutant proteins.

The expression of the Bcl-2 M157I/C158A/C229V single cysteine mutants was measured by immunoblotting, and only those expressed at the level of wild type were used for subsequent functional and labelling experiments. All of the mutants met this criterion except mutants I173C, A174C and M177C, which showed little or no expression after the first passage post-infection (This result was replicated in three separate infections). Figure 3.2 shows a representative western blot of Bcl-2 using cell lines at the third passage after infection. For the mutant I173C, a small amount of expression was detected, but little or no expression was seen after this passage. The expression of mutants V156C and S167C have slightly lower expression in this experiment, but further replicates indicated that these proteins were expressed at wild type levels.

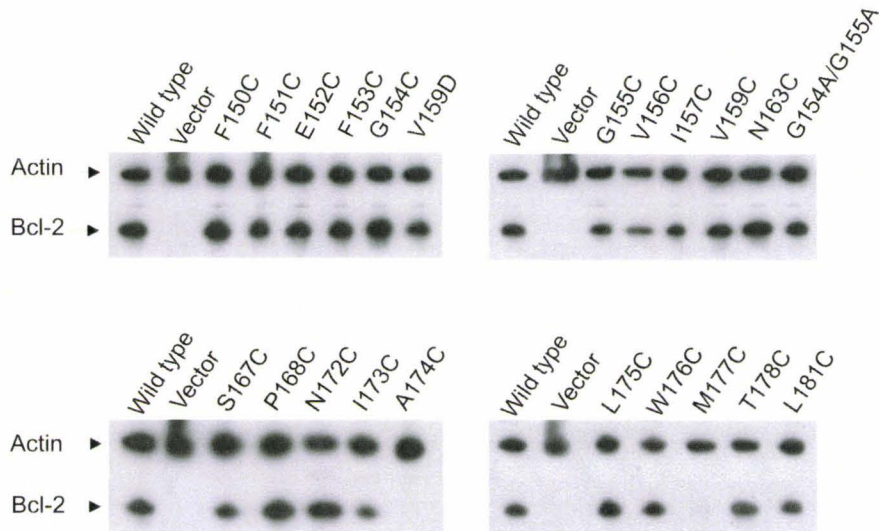


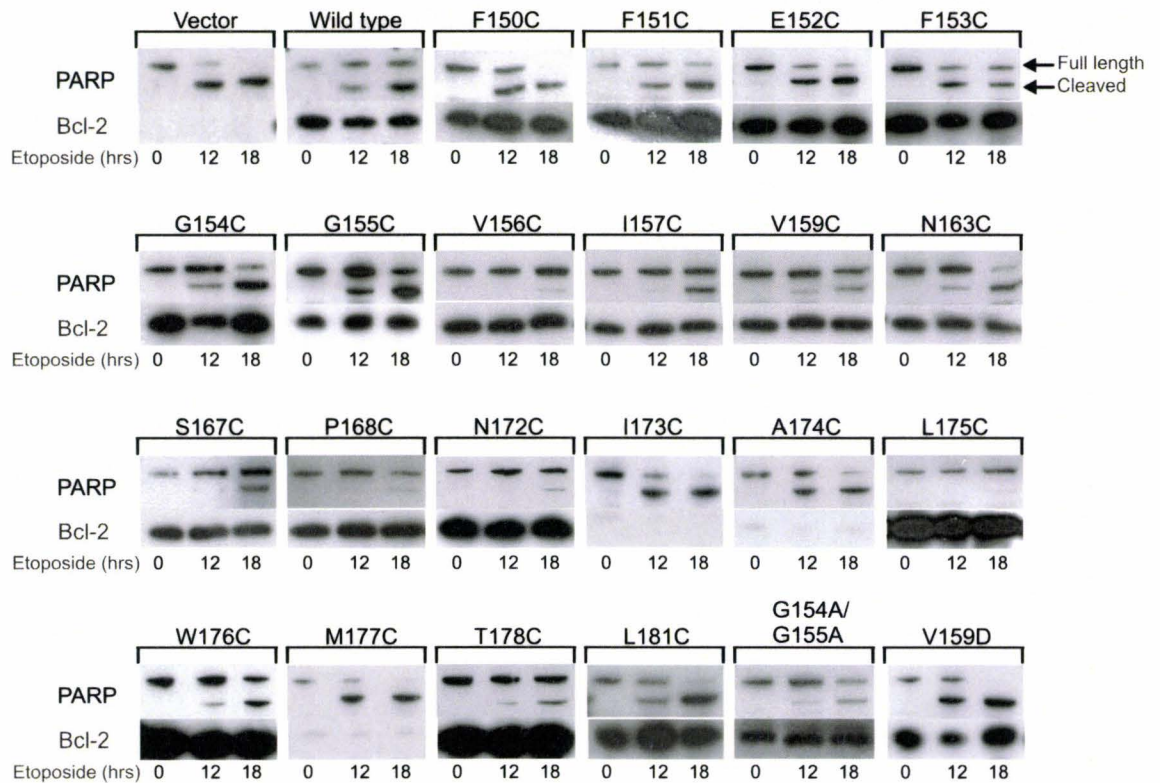
Figure 3.2 Expression of Bcl-2 mutant proteins in rat 1 myc ERTM fibroblasts after retroviral infection Rat 1 myc ERTM fibroblast cell lines were infected with retroviruses encoding mutants of Bcl-2 M157I/C158A/C229V, using the viral packaging cell line Phoenix-Eco and selected for hygromycin resistance. Whole cell lysates were prepared by harvesting cells and lysing in hot 1% SDS lysis buffer. 8µg total protein was analyzed by SDS-PAGE and immunoblotted for Bcl-2 and actin. The expression of each mutant protein was compared to wild type Bcl-2 and empty vector-infected cells. Mutants are designated by the identity and position of the endogenous residue replaced with cysteine. Actin was used as a loading control.

3.2 Bcl-2 mutant proteins expressed in rat 1 myc ERTM fibroblasts exhibit anti-apoptotic function

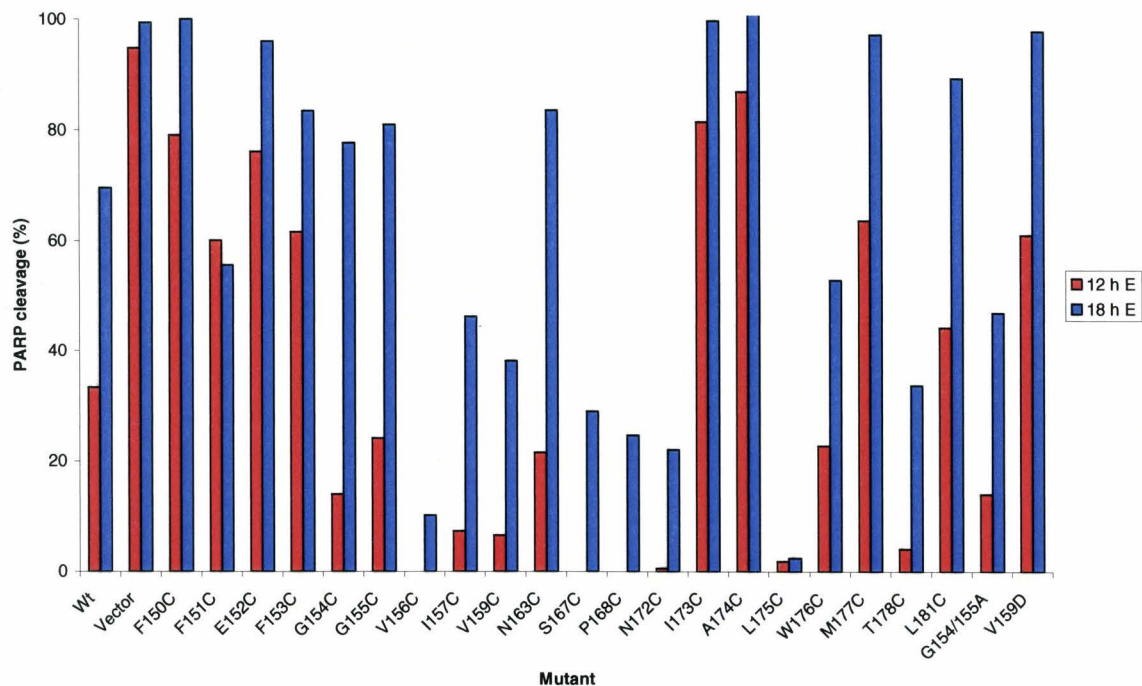
The anti-apoptotic function of each Bcl-2 mutant was tested in rat 1 myc ERTM cells. PARP, poly(ADP-ribose) polymerase-1, is a nuclear enzyme which is cleaved by caspases 3 and 7 during apoptosis generating a characteristic subfragment that can be distinguished from the full length protein by SDS-PAGE (Chiarugi and Moskowitz, 2002). The appearance of a cleavage product detected by quantitative immunoblotting after SDS-PAGE was used to identify cells undergoing apoptosis. Figure 3.3 shows representative immunoblots and bar graphs of mean PARP cleavage values for each mutant, after either exposure to etoposide or serum starvation. In wild type Bcl-2 expressing cells, 18 hours of etoposide treatment caused cleavage of 70 +/- 2% (average +/- standard deviation) of cellular PARP, whereas treatment of vector control cells caused 99 +/- 4% PARP cleavage (Table 5). After 48 hours of serum starvation-induced apoptosis, 49 +/- 9% of PARP was cleaved in wild type Bcl-2 expressing cells compared to 82 +/- 4% cleavage in vector control cells (Table 6). A few mutants have more cleavage at the middle time point than the later one, probably due to subsequent cleavage of cleaved PARP by other apoptotic proteases in the cell. Tables 4-7 show the results of the one-way analysis of variance (ANOVA) comparing PARP cleavage for cells expressing wild type Bcl-2, vector control or mutants from three replicate experiments. All of the single cysteine mutants, which were expressed at the level of wild type, had at least some anti-apoptotic function, except F150C which had PARP cleavage similar to the vector control cells in both treatments. The low or non-expressing mutants, N173C,

A174C and M177C, also functioned like vector, as expected. The two additional Bcl-2 mutants designed to investigate function, V159D and G154A/G155A, were chosen for further investigation because one, V159D, was less functional than wild type (hypo-functional), whereas the other, G154A/G155A, was more functional (hyper-functional).

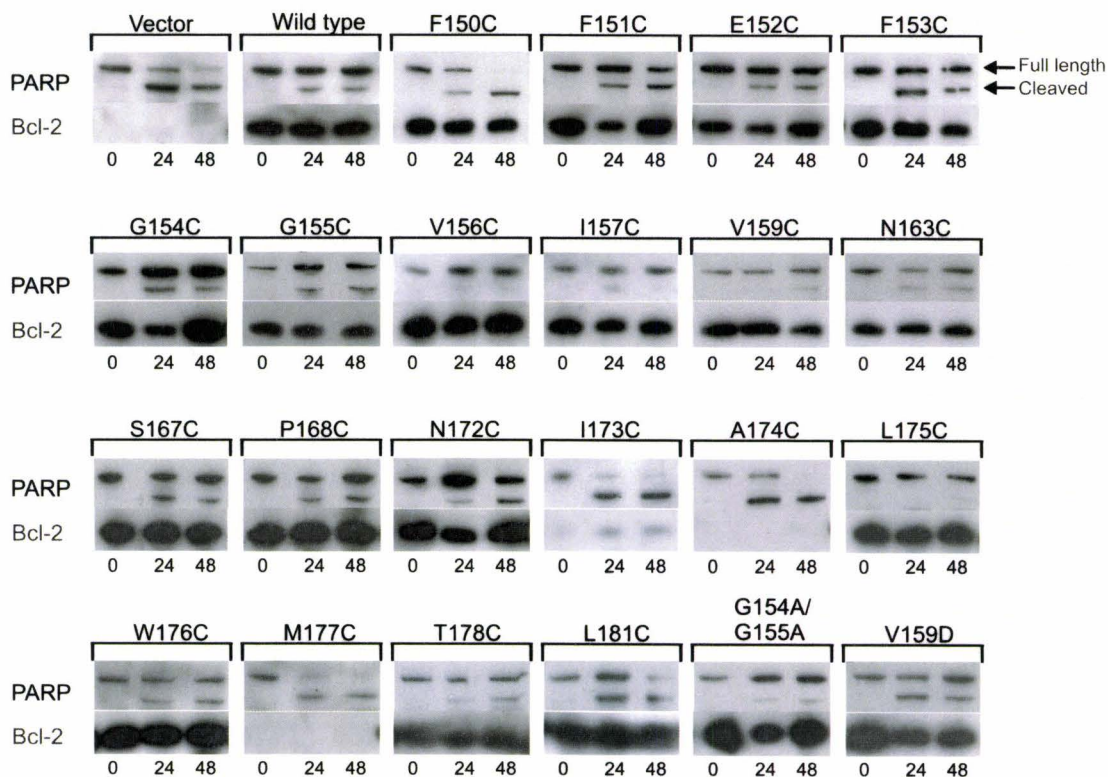
a)



b)



c)



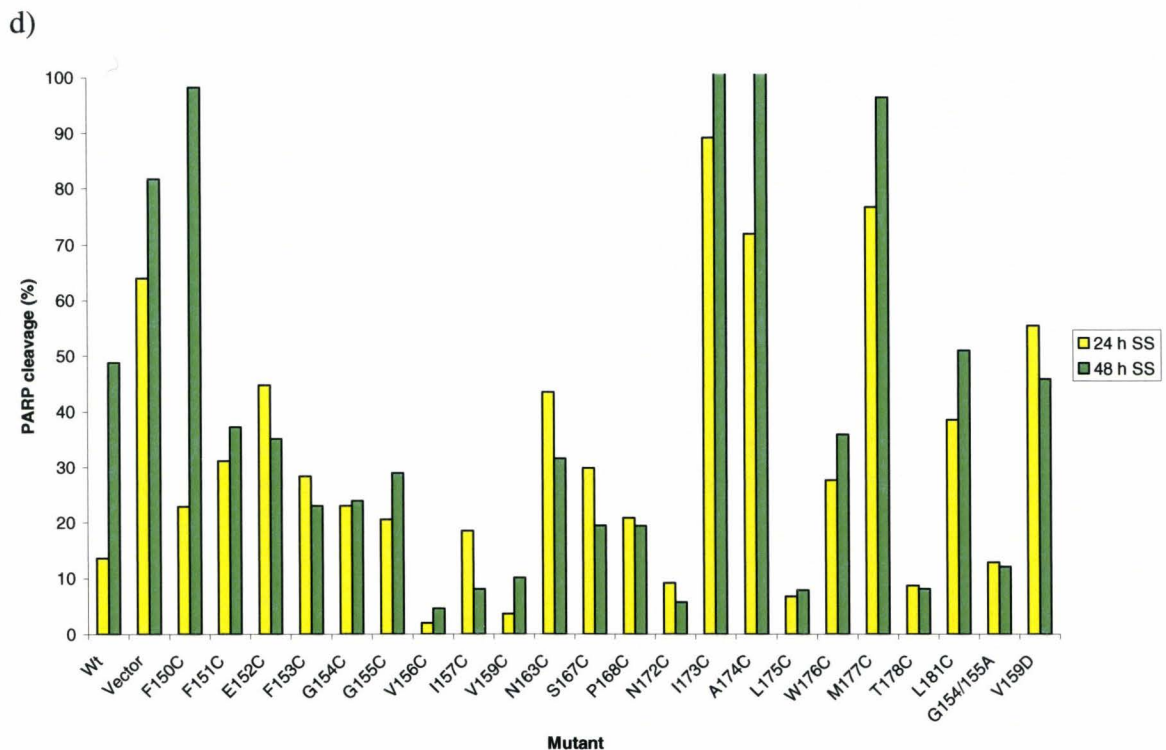


Figure 3.3 Anti-apoptotic function of Bcl-2 mutant proteins in rat 1 myc ERTM fibroblasts after treatment with etoposide or serum starvation A PARP cleavage assay was used to determine the anti-apoptotic activity of Bcl-2 in rat 1 myc ERTM fibroblasts. PARP, poly(ADP-ribose) polymerase-1, is a nuclear enzyme which is cleaved by caspases 3 and 7 during apoptosis (Chiarugi and Moskowitz, 2002); the resulting fragment can be detected by immunoblotting after SDS-PAGE. Fibroblasts infected with an empty vector or expressing wild type or mutant Bcl-2 proteins were treated with either (a and b) 6 μ M etoposide for 0, 12 or 18 hours, or (c and d) 0.03% FBS for 0, 24 or 48 hours. All cells were also treated with 4-hydroxytamoxifen according to the rationale explained in the text. After treatment, cells were harvested and lysed in hot 1% SDS lysis buffer. Samples containing of 8 μ g total protein were electrophoretically separated on SDS-PAGE and analyzed by immunoblotting for PARP and Bcl-2 (a and c). Films from western blots were scanned and apoptosis was measured by comparing the volume of intensity of each full length PARP band with the volume of intensity in each cleavage product band. The percent of cleavage at each time point was calculated and ANOVAs

were conducted on three replicate experiments. b) and d) show graphical representations of the mean PARP cleavage values at each time point in etoposide (12h E or 18h E) and serum starvation conditions (24h SS or 48h SS), respectively. Where no bars are present, the values were zero, indicating the absence of PARP cleavage. Pooled standard deviation values for each time point are reported in Tables 4-7.

Table 4 One-way ANOVA comparing PARP cleavage after 12 hours of etoposide treatment

Protein	N	Mean	StDev	Individual 95% CIs For Mean Based on Pooled StDev
Wild Type	3	33.24	9.29	(--*--)
Vector	3	94.74	1.25	(--*--)
F150C	3	79.10	19.19	(----*)
F151C	3	60.03	6.72	(--*--)
E152C	3	76.17	11.05	(----*)
F153C	3	61.56	5.94	(----*)
G154C	3	14.01	9.72	(--*--)
G155C	3	24.13	11.37	(----*)
V156C	3	-0.96	1.31	(----*)
I157C	3	7.34	5.65	(--*--)
V159C	3	6.56	5.52	(--*--)
N163C	3	21.54	9.23	(--*--)
S167C	3	-0.85	1.69	(----*)
P168C	3	-2.45	1.22	(--*--)
N172C	3	0.55	0.65	(--*--)
I173C	3	81.37	21.17	(--*--)
A174C	3	86.71	11.76	(----*)
L175C	3	1.80	1.37	(----*)
W176C	3	22.74	13.48	(--*--)
M177C	3	63.58	20.78	(--*--)
T178C	3	4.09	3.76	(--*--)
L181C	3	44.16	3.49	(----*)
G154/5A	3	14.00	7.18	(--*--)
V159D	3	60.89	11.18	(--*--)

Pooled StDev = 10.09
P value 0.000

PARP Cleavage (%)

Table 5 One-way ANOVA comparing PARP cleavage after 18 hours of etoposide treatment

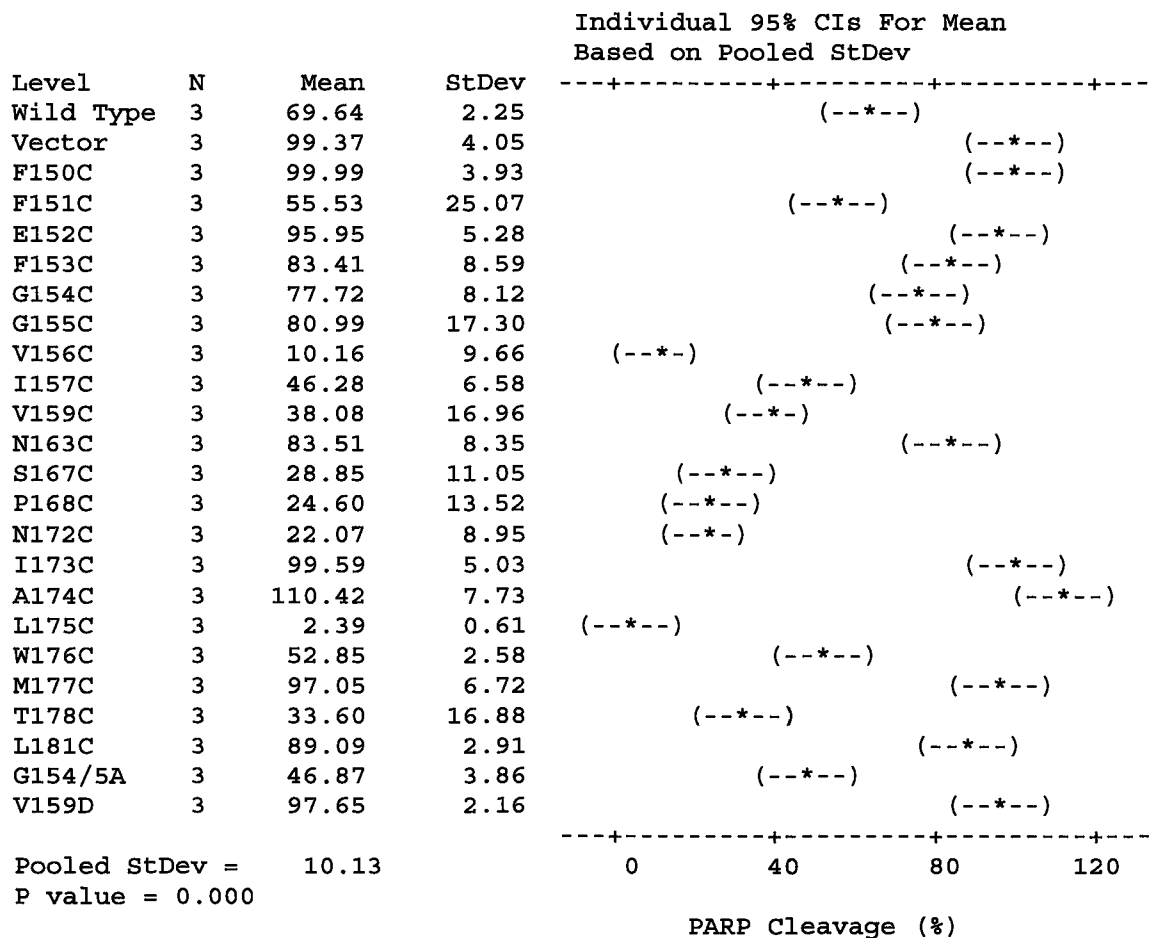
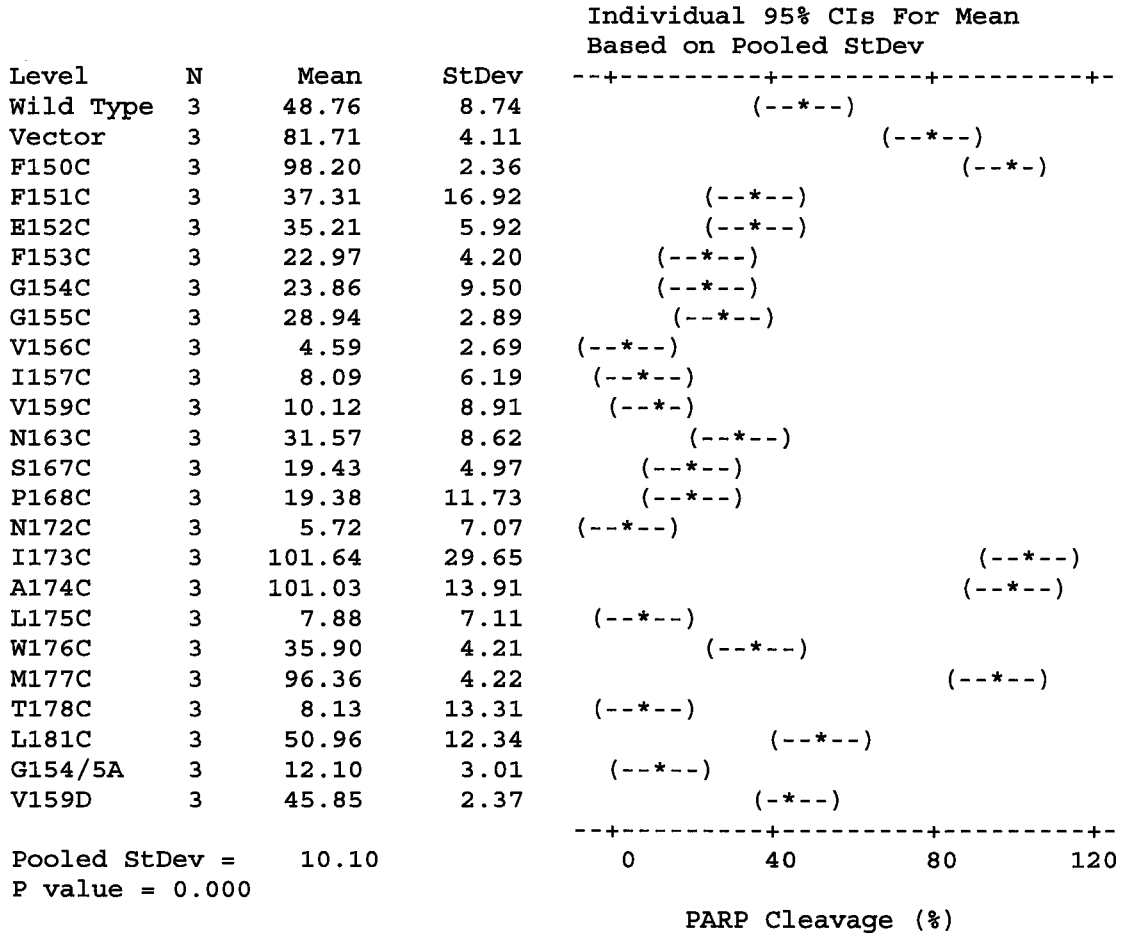


Table 7 One-way ANOVA comparing PARP cleavage after 48 hours in serum starvation conditions



3.3 Bcl-2 membrane topology after apoptosis, assayed by IASD labelling of single cysteine mutants

High expressing, functional Bcl-2 mutants were used to investigate the membrane topology of Bcl-2 during apoptosis, by IASD labelling. Using this assay system, we have demonstrated that eight of the fourteen cysteine residues introduced into helix $\alpha 5$ or $\alpha 6$ are at least partially protected from IASD labelling after incubation with etoposide or serum starvation. Figure 3.4a) shows representative western blots of the labelling reactions for wild type Bcl-2 and each mutant, where the shift in mobility of the labelled protein has been resolved using isoelectric focusing (IEF) gels. A schematic interpretation of the local membrane topology of Bcl-2 suggested by the result is also shown for each functional mutant. In the absence of IASD labelling, designated Time 0 in the Figure, wild type Bcl-2 focused into a single band under all conditions. After 10 minutes of labelling in untreated cells, the Bcl-2 band shifted downward due to the labelling of one cysteine residue (C158) resulting in a change in the isoelectric point of the protein and migration to a lower pH in the gel. The second endogenous cysteine (C229) located in the carboxyl-terminal transmembrane domain served as an internal positive control, as it was protected from labelling by the membrane except when labelled in detergent, in which case a “double” shift occurred due to membrane solubilization. After etoposide or serum starvation treatment, wild type Bcl-2 was only partially shifted after 10 minutes of IASD exposure. This suggests that C158 was protected from labelling by the membrane, as recently published by our laboratory (Kim et al., 2004). The amount of unlabelled protein after ten minutes of incubation in IASD was measured on

immunoblots of the IEF gels for both treated and untreated cells. In the latter, 10 +/- 6% (mean +/- standard deviation) of wild type Bcl-2 was unlabelled (protected by the bilayer) compared to 71 +/- 7% after etoposide and 72 +/- 8% after serum starvation. Thus, in both treatment conditions the amount of unlabelled protein was significantly higher than in untreated cells. A similar analysis was performed for each of the single cysteine mutants, for which only a single band shift was possible (Control experiments demonstrated that no band shift was detected in a mutant in which both cysteines had been replaced by valine). By contrast, the V159D and G154A/G155A mutants contain both endogenous cysteine residues; thus, the two shifts detectable in the wild type protein were possible after IASD labelling.

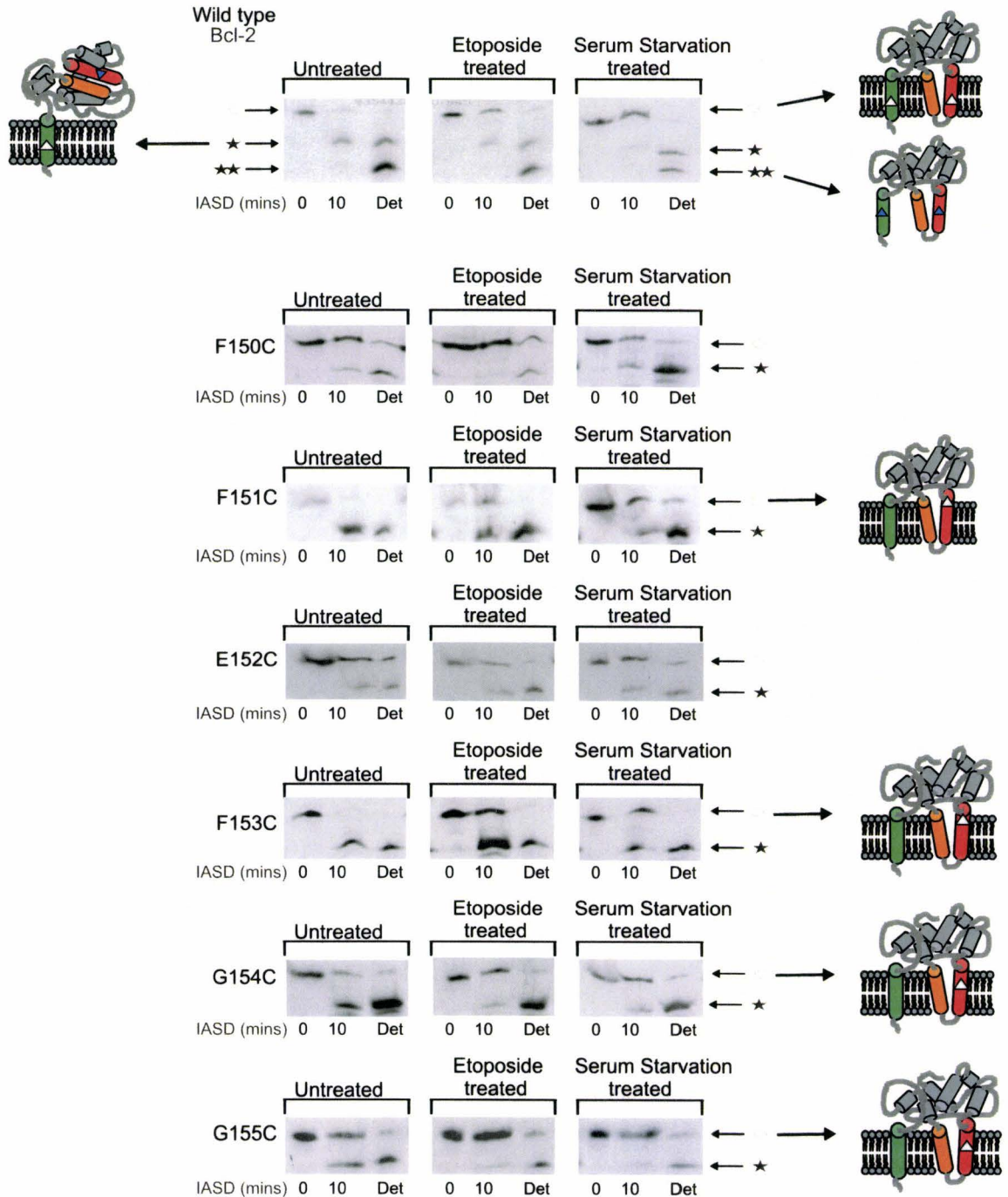
The results from three replicate experiments for each mutant were analyzed by one way ANOVA to compare the IASD labelling results of the wild type with the Bcl-2 mutant proteins. Tables 8-10 show the results of the ANOVA for the measured amount of unlabelled protein in both untreated cells and after each of the treatments. In Figure 3.4 b)- d) graphical representations of the mean amount of unlabelled protein for each mutant compared to the wild type result are shown, with the mutants grouped into separate categories (hypo-functional, wild type function or hyper-functional) as described in Section 2, Tables 4-7 and summarized in Table 13. However, because hypo-function of a mutant may be due to misfolding, no conclusions about membrane topology can be drawn from the IASD labelling data of this set.

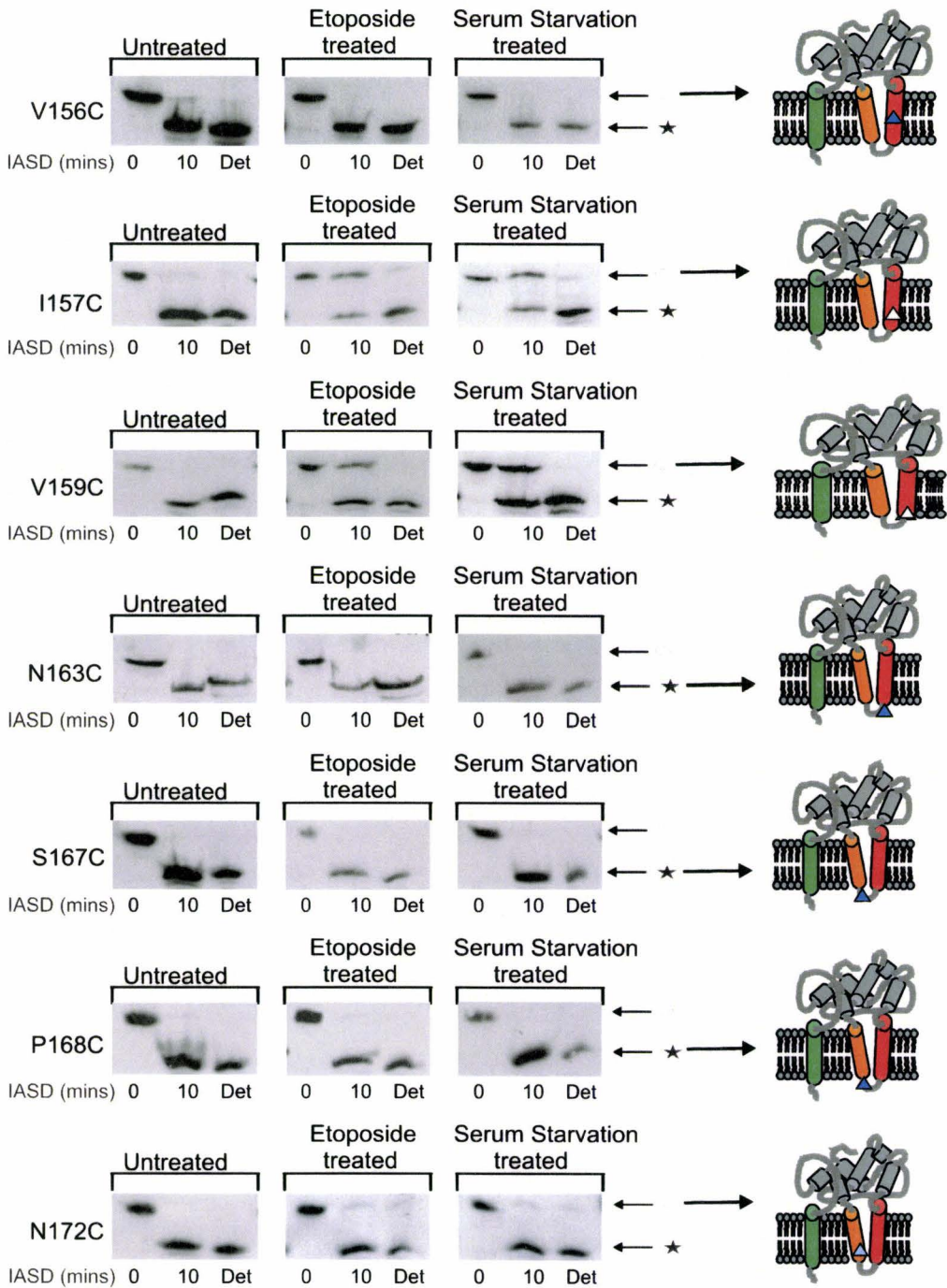
Although most mutants were completely accessible to IASD labelling in untreated cells, in the G155C mutant a significant amount of unlabelled protein was observed in

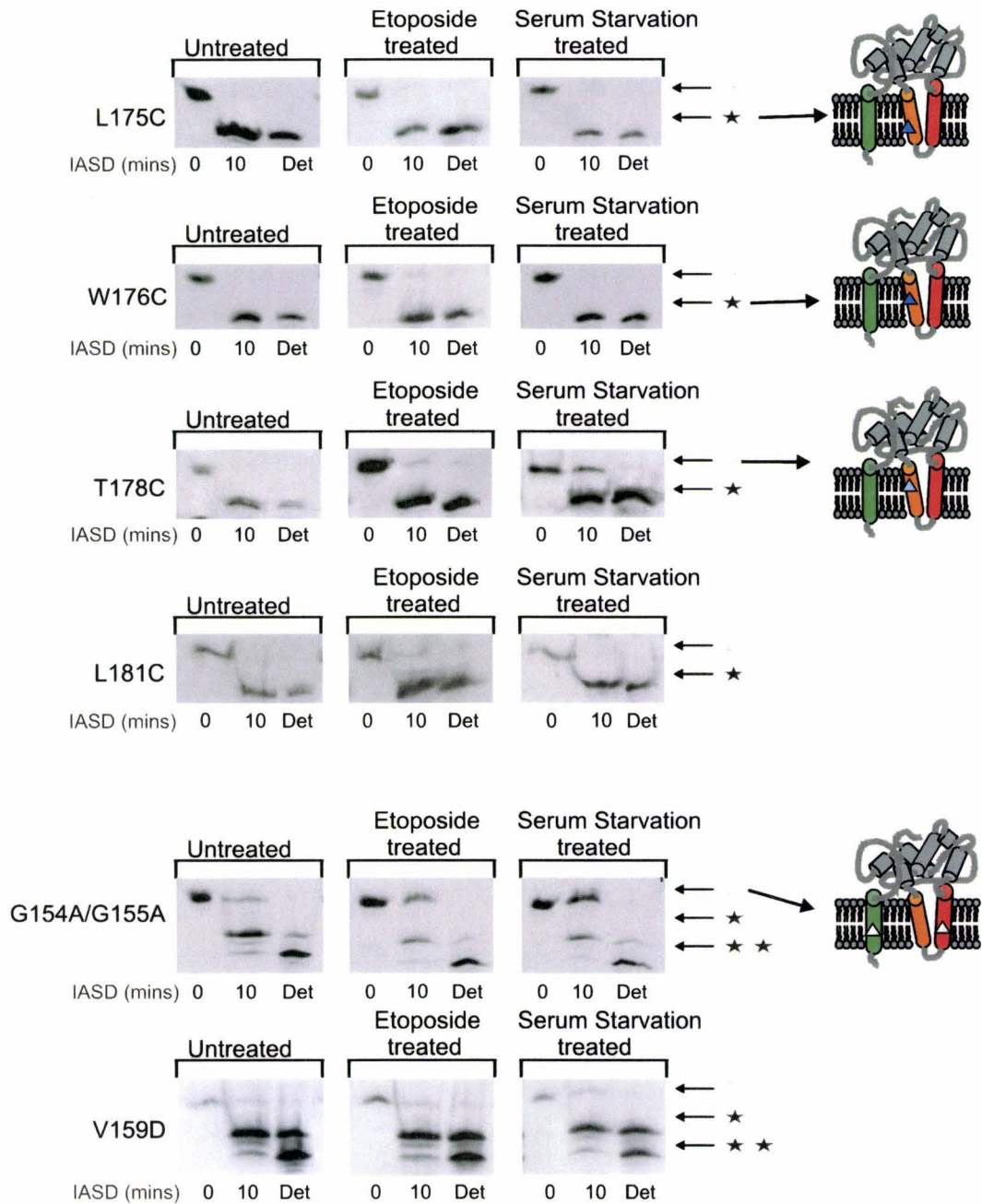
both untreated and treated cells. To correct for this variation between mutants, the difference in the amount of unlabelled protein between untreated and treated cells was calculated for each mutant, and subjected to one way ANOVA. Tables 10 and 11 illustrated the results of the ANOVA for this *net* amount of unlabelled protein after each treatment. The results of this ANOVA were used to designate mutants as protected, partially protected or accessible to IASD, as summarized in Table 13, and for the construction of the topology map shown in Figure 3.5a). For the purposes of our analysis, if the 95% CI for a mutant overlapped with the 95% CI of the wild type protein, then the mutant was considered to be protected from labelling. We defined a mutant as partially protected if the mean amount protected fell below the wild type confidence interval, but above zero. Means of zero or less were considered accessible residues. The data show that discontinuous regions of both the $\alpha 5$ and $\alpha 6$ helices were at least partially protected after the induction of apoptosis. Mutants of the $\alpha 5$ helix F153C, G154C and I157C all showed similar protection from labelling as seen in the wild type (white triangles in Figure 3.5) for both treatment conditions. F151C, G155C and V159C were protected like wild type after etoposide and were only partially protected during serum starvation (white triangles in Figure 3.5). Mutants N172C and T178C in $\alpha 6$ were partially protected from labelling in both treatments (light blue triangles in Figure 3.5). The mutants in the loop between the two helices (N163C, S167C and P168C) as well as V156C in $\alpha 5$ and L175C and W176C in $\alpha 6$ were all fully accessible (dark blue triangles in Figure 3.5). The endogenous C158 residue in the hyper-functional G154A/G155A mutant was partially protected after etoposide treatment but showed protection similar to wild type after serum

starvation. The C158 residue in the hypo-functioning V159D mutant was partially protected after both treatments.

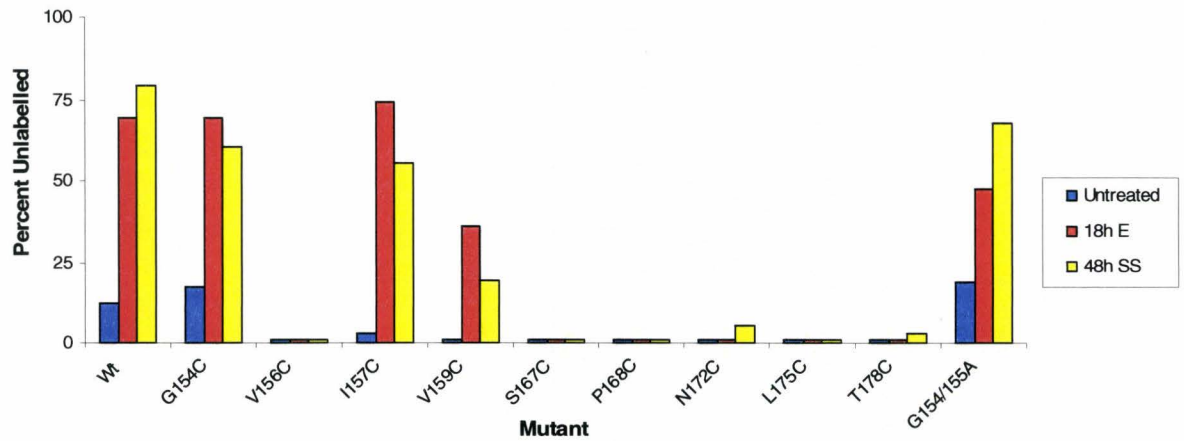
a)



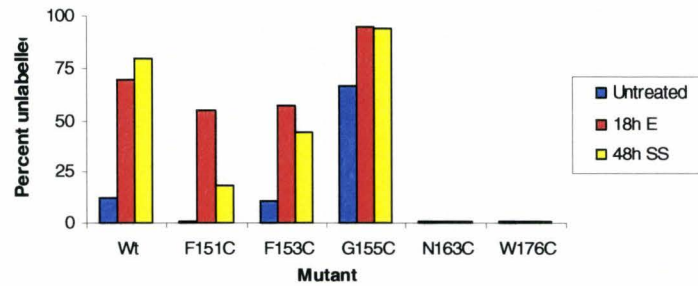




b) Hyper-functional



c) Wild type function



d) Hypo-functional

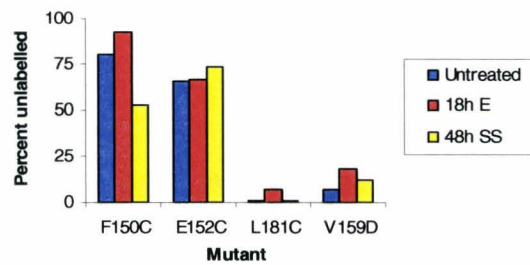


Figure 3.4 Isoelectric focusing of IASD labelled wild type and mutant Bcl-2 proteins in untreated, etoposide- or serum starvation-treated cells

Cells were lysed by nitrogen cavitation, nuclei were removed and both heavy and light membrane fractions were isolated by ultracentrifugation. Labelling was done in cell buffer with 4M Urea at pH 8. Samples were incubated in 16 mM IASD for 0 and 10 minutes, as well as in 2% Triton X-100 (Det) for 10 minutes, were indicated. DTT (160 mM) was added to each sample to stop labelling. CHAPS (4%) and IGEPAL (NP40, 8%) were added to solubilize membranes prior to sonication. 25µg of total protein was loaded per lane. Proteins were transferred to PVDF membranes and immunoblotted with a poly-clonal Bcl-2 antibody. Films were scanned and the extent of labelling after incubation in IASD was measured. The percent of unlabelled protein after 10 minutes of IASD labelling was calculated and the results of three replicate experiments subjected to an ANOVA. Representative Immunoblots of all the proteins analyzed for gel shift after IASD labelling are shown in a) for untreated, etoposide- or serum starvation-treated cells. The top band in each lane represents unlabelled protein (°). A single shift downward denotes one labelled cysteine residue (*), a second shift denotes two labelled cysteine residues (**). Wild type Bcl-2, V159D and G154A/G155A have two cysteine residues. In untreated cells, the endogenous cysteine, C229, located in the c-terminal transmembrane domain of wild type Bcl-2, is protected from labelling by the membrane, whereas C158 located in helix $\alpha 5$ is labelled by IASD, resulting in a one shift downward of the Bcl-2 band (*). After the induction of apoptosis, C158 is protected from labelling, suggesting helix $\alpha 5$ is inserted into the membrane. In the detergent control, both cysteines should be labelled (**). The schematic diagrams show one interpretation of the membrane topology suggested by the data; other alternatives are discussed in the text. Triangles represent the position of each residue; White indicates protected, light blue indicates partially protected and dark blue indicate accessible residues. b), c) and d) are graphical representation of the mean values of unlabelled protein before and after treatment, with the mutants grouped according to degree of anti-apoptotic function (hyper-functional, wild type function or

hypo-functional, respectively) as discussed in the text. The pooled standard deviation values for each time point are reported in Tables 8-10.

Table 8 One-way ANOVA comparing protection from IASD labelling of wild type and Bcl-2 mutant proteins in untreated cells

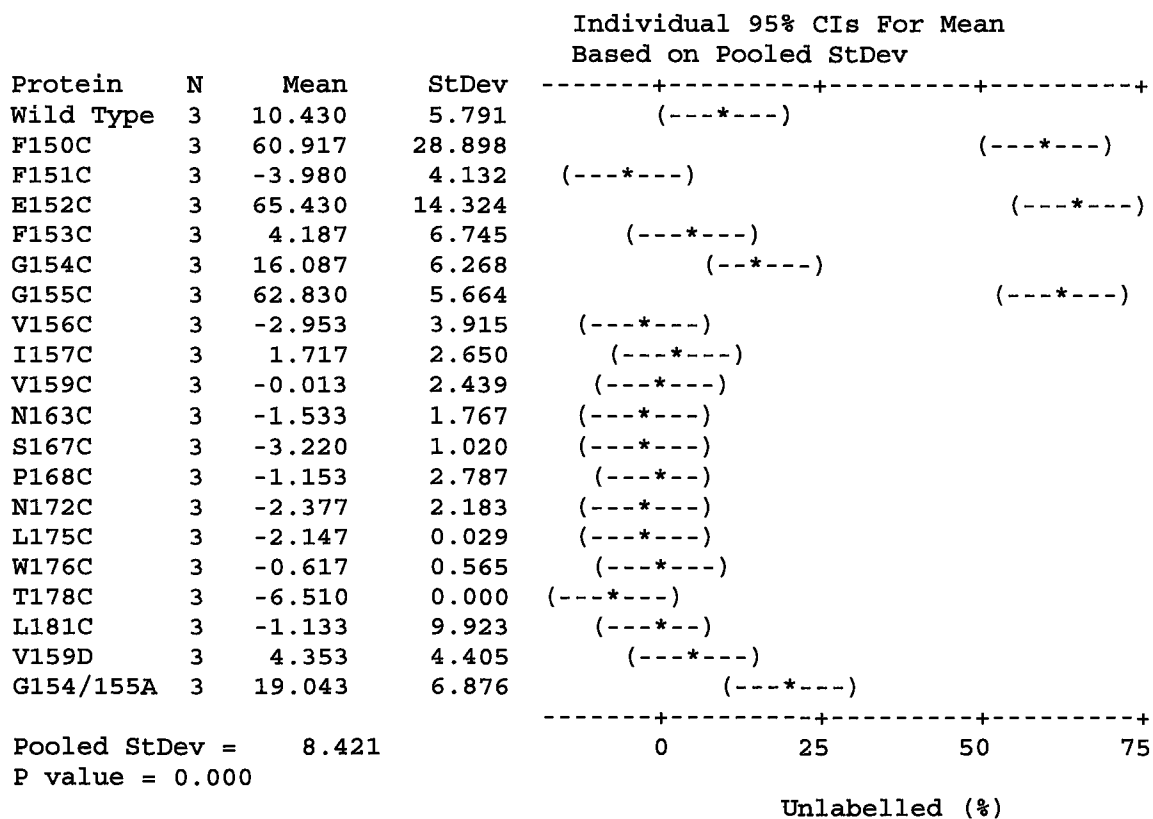


Table 9 One-way ANOVA comparing protection from IASD labelling of wild type and Bcl-2 mutant proteins after 18 hours of etoposide treatment

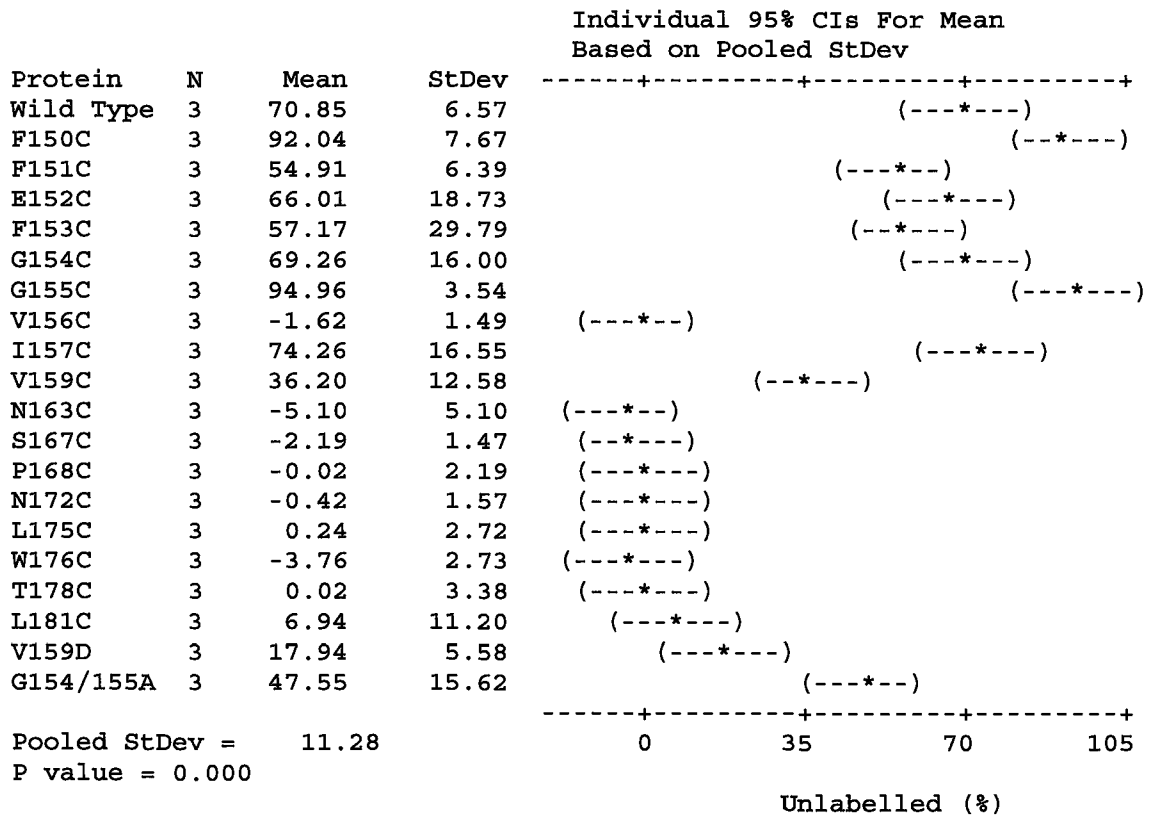


Table 10 One-way ANOVA comparing protection from IASD labelling of wild type and mutant Bcl-2 proteins after 48 hours of serum starvation

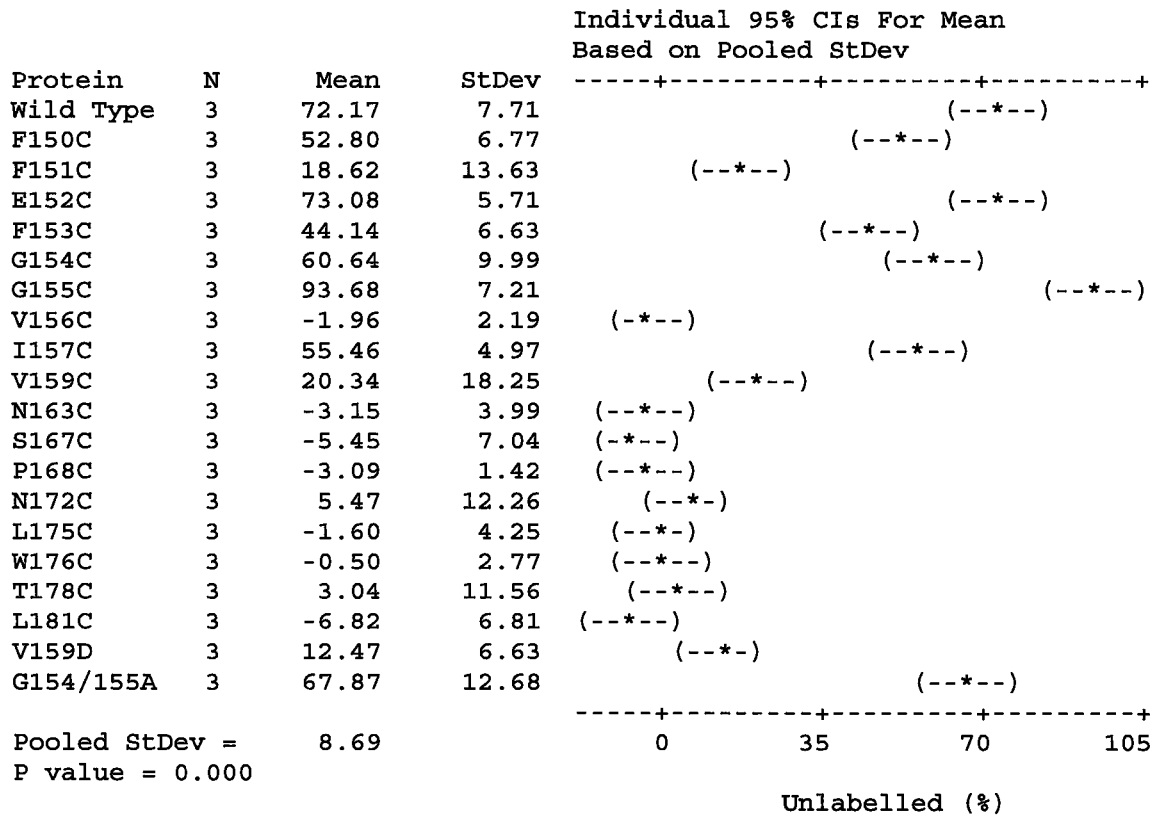


Table 13 Summary of degree of anti-apoptotic function and protection from IASD labelling of wild type and Bcl-2 mutants

Protein	Function	Protected from IASD labelling? (net)
Wild Type	Wild Type	Yes
F150 C	None	Pt
F151 C	Wild Type	Yes ^E
E152 C	Hypo ^{SS}	No
F153 C	Wild Type ^{SS}	Yes
G154 C	Hyper	Yes
G155 C	Wild Type	Yes ^E
V156 C	Hyper	No
I157 C	Hyper	Yes
V159 C	Hyper	Yes ^E
N163 C	Wild Type	No
S167 C	Hyper	No
P168 C	Hyper	No
N172 C	Hyper	Pt
I173 C	None	-
A174C	None	-
L175 C	Hyper	No
W176 C	Wild Type	No
M177 C	None	-
T178 C	Hyper	Pt
L181 C	Hypo	Pt
G154A/ G155A	Hyper	Yes ^{SS}
V159D	Hypo	Pt

{ Helix α 5
 { Helix α 6
 { Additional Mutants

Wild Type^{SS} : hypo-functional after etoposide treatment, wild type function after serum starvation

Hypo^{SS} : no function with etoposide, hypo-functional after serum starvation

- : expression was too low to detect Bcl-2 expression after IASD labelling

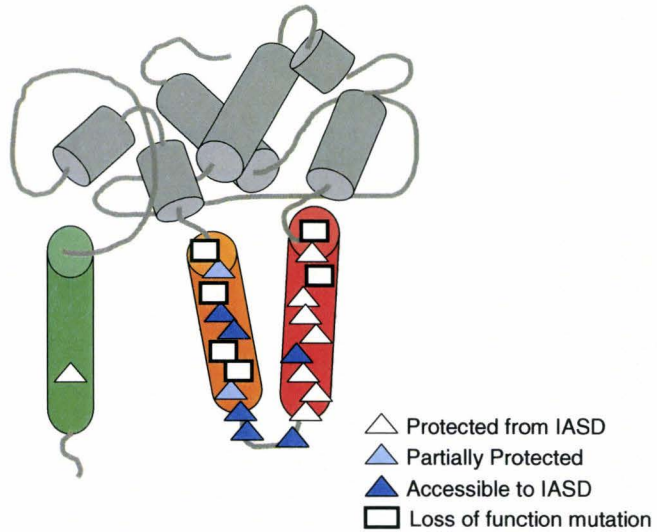
Yes^E: protected from IASD labelling like wild type after etoposide, partially protected after serum starvation

Yes^{SS}: partially protected from IASD labelling after etoposide, protected like wild type after serum starvation

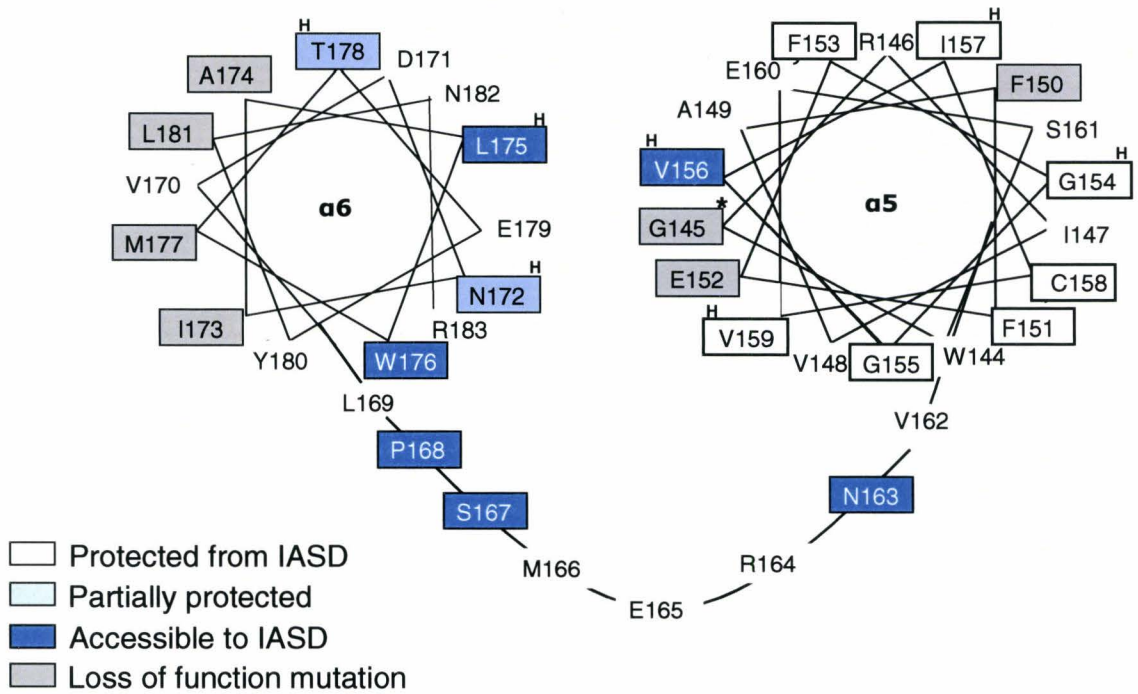
3.4 IASD labelling data suggests that Bcl-2 changes conformation after the induction of apoptosis, whereby helices $\alpha 5$ and $\alpha 6$ insert into the membrane

The IASD labelling data was used to construct a map of the protected and accessible areas of the protein. Figure 3.5 shows the location of each residue in four schematic diagrams and the status of labelling associated with each after treatment. Figure 3.5a) shows the discontinuous protection pattern in each helix. Figure 3.5b) shows on helical wheel diagrams that the accessible residue in the middle of $\alpha 5$ (V156C) is on the same side of the helix as the charged residue E152C and the side opposite to protected residues at C158 and G154C. On helix $\alpha 6$, mutants which caused loss of function, I173C, A174C and M177C are on one side of the helix, opposite to the accessible residues L175C and W176C. One interpretation of these data is that only the $\alpha 5$ helix of Bcl-2 is protected by lying parallel to the membrane (Figure 1.4), but this topology would not explain the protected residues on helix $\alpha 6$. Alternatively, a partial or shallow insertion of both helices is possible, similar to the shallow insertion of the pore forming region of diphtheria toxin (Rosconi and London, 2002). However, in this case, the observed accessibility of residues in the adjoining loop between $\alpha 5$ and $\alpha 6$ and the protection of residues at the base of the helices (F153C and T178C) is not predicted. The model most compatible with all the data is one in which the $\alpha 5$ and $\alpha 6$ helices insert and span the membrane, causing the loop between the helices to be situated on the opposite side of the membrane. Figure 3.5c) shows the change in topology of Bcl-2 during apoptosis, where Bcl-2 changes from a single spanning membrane protein to one with multiple transmembrane domains.

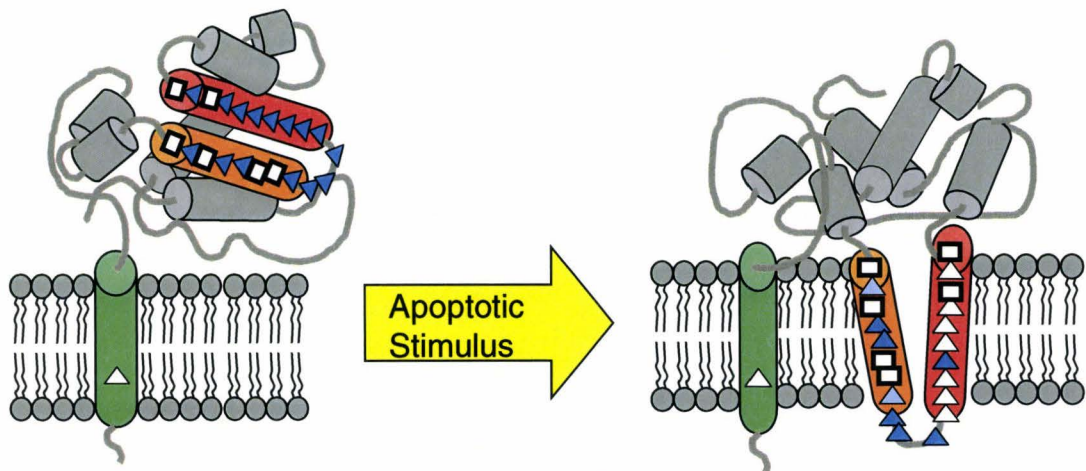
a)



b)



c)



d)

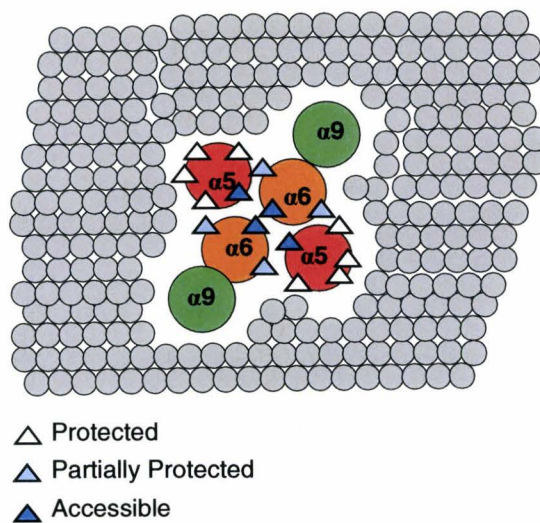


Figure 3.5 Schematic representations of residues which are protected from IASD labelling after etoposide or serum starvation treatment and model of predicted membrane topology a) shows the IASD labelling data from functional mutants displayed in a schematic in which protected positions are represented by white triangles, partially protected residues by light blue triangles and accessible residues by dark blue triangles. White boxes with dark outlines represent the loss of function mutations. b)

shows helical wheel diagrams of helices $\alpha 5$ and $\alpha 6$ of Bcl-2 as well as the loop regions between the helices. Each box represents the position of a single cysteine residue. The white and light blue boxes represent protected and partially protected residues, respectively. The dark blue boxes indicate accessible residues. The grey boxes represent loss of function mutations and hyper-functional mutants are indicated with an H above the box. The mutation G145A(*) in wild type Bcl-2 also causes loss of anti-apoptotic function (Yin et al., 1994). c) shows a schematic diagram of the change in topology of Bcl-2 in a plane parallel to the membrane. In this model, the $\alpha 5$ and $\alpha 6$ helices of Bcl-2 insert and span the membrane after induction of apoptosis, resulting in protection from IASD labelling of certain residues within the membrane spanning regions. d) shows a model of a homodimer of Bcl-2, during apoptosis, in which helices $\alpha 5$ and $\alpha 6$ of both are inserted into the membrane. This model is consistent with the data in which certain residues in helices $\alpha 5$ and $\alpha 6$ remain accessible to IASD, post membrane insertion. An aqueous environment could be created between helices in close proximity, resulting in IASD labelling of residues within the membrane. The grey circles represent membrane lipids and other membrane components. The larger green, red and orange circles correspond to helices $\alpha 9$, $\alpha 5$ and $\alpha 6$, respectively. The triangles represent positions of protected, partially protected and accessible residues compatible with this topology.

In cells, Bcl-2 exists in homodimers, both before and after the induction of apoptosis. Figure 3.5d) shows a schematic of a homodimer of Bcl-2 where both components are in a membrane spanning topology after the induction of apoptosis. The side-by-side arrangement of the helices within the membrane, of both members of the homodimer, could create aqueous environments between them, thereby allowing IASD to label residues situated within a membrane spanning region, as elaborated in more detail in the Discussion chapter.

CHAPTER 4: DISCUSSION

4.1 Expression of Bcl-2 Mutant Proteins

The expression of most mutant Bcl-2 proteins did not differ from wild type. It is important to have equivalent expression among proteins because the degree of protection by Bcl-2 is proportional to its intracellular concentration (Huang et al., 1997). The lower expression of three mutants (I173C, A174C and M177C), may be related to changes in the character of the amino acid and the effect of this change on the local environment that could cause inappropriate folding, thereby decreasing the stability of the protein. In all three cases, hydrophobicity was altered by these mutations: isoleucine is very hydrophobic, alanine and methionine are weakly hydrophobic, whereas cysteine is moderately hydrophobic (between isoleucine and alanine). Changing from isoleucine to the less bulky cysteine decreases the hydrophobic character of this area of the protein, whereas changing alanine (smaller than cysteine) or methionine (larger than cysteine) to cysteine increases the hydrophobicity slightly. However, in helix $\alpha 5$, the change from isoleucine to cysteine did not have the same result. The mutant I157C was expressed at an adequate level and functioned slightly better than wild type. This suggests that the mutation in helix $\alpha 6$ caused low expression as a result of a change on the local environment, not just the nature of the change.

Another similarity shared by these mutant proteins that were expressed at low levels is that all the residues are on one side of helix $\alpha 6$ (Figure 3.5). This suggests that this area of Bcl-2 is important for protein stability since mutations cause low expression. The NMR structure of Bcl-2 shows that helices $\alpha 5$ and $\alpha 6$ are surrounded by amphipathic

helices and protected in a hydrophobic pocket (Petros et al., 2001). In cells, this side of helix α_6 may be important for the correct assembly of this pocket or may help to keep the pocket intact, once folded.

4.2 Anti-apoptotic Function of Bcl-2 Mutants

There was large variation in the anti-apoptotic function of the Bcl-2 mutants. In general, there was no correlation between the nature of the change of residue and the effect on the function of the protein, but mutations in certain areas had similar effects on function.

Since Bcl-2 exists in two different conformations, it is likely that aqueous and membrane interactions are required for stabilization in both forms. Thus, the functional effect of a change in hydrophobicity would depend on where the mutation is and which configuration is stabilized. If the resting, tail anchored conformation were stabilized, the function might decrease. For example, if a mutation increased the hydrophobicity of helices α_5 and α_6 , these two helices could become “stuck” within the hydrophobic pocket of Bcl-2, because greater energy would be needed to facilitate the change to the active conformation. Thus, the protein would have lower anti-apoptotic function. Conversely, if the active, polytopic conformation were stabilized, such a mutant may become more efficient in inhibiting apoptosis, as shown in studies with a Bcl-xL mutant in which increased mobility in the second transmembrane domain resulted in hyper-function (Asoh et al., 2000). Alternatively, a mutation may stabilize critical protein-protein interaction between Bcl-2 and binding partners such as Bax, resulting in enhanced function.

Both increases and decreases in hydrophobicity, in N172C and V156C, respectively, resulted in increased anti-apoptotic function. This shows that the effect of the change on the local environment had more of an effect on function than the nature of the change alone. In addition, the same amino acid substitution had a different effect on different positions in the protein. For example, the change from glycine to cysteine caused no change in function at position G155 but increased the function of the protein in position G154. Interestingly, the double mutant G154A/G155A also caused an increase in the function of the protein. This suggests that the change at position G154 has a more significant effect on function than G155. Mutations to the residue V159 also caused differing results. The single cysteine mutant V159C resulted in a hyper-functional mutant; when V159W was the only mutation in the protein, there was a slight decrease in function, whereas the introduction of a charged residue into the position, V159D, caused a significant decrease in function.

One trend identified in the effect of mutations made to Bcl-2 was that substitutions in certain areas of each helix resulted in similar changes in Bcl-2 function, independent of the nature of the change. Many of the single cysteine mutants in helix $\alpha 5$ are hyper-functional (Table 13), even though the mutations cause both increases and decreases in hydrophobicity. This could be due to the proximity of these residues to position C158, as the addition of a cysteine may compensate for the removal of the endogenous residue. Mutants with cysteines proximal to C158, such as I157C and V159C, had increased anti-apoptotic function, whereas more distal cysteines, F150C and L181C, had decreased function. In addition, mutations on one side of helix $\alpha 6$, facing

toward helix $\alpha 5$ according to the helical wheel diagrams, were hyper-functional, whereas mutations on the opposite side caused decreased expression. Hyper-functional mutants N172C, L175C and T178C reside on the same side of helix $\alpha 6$ as two charged residues, D171 and E179 (Figure 3.5b). This suggests that mutations in the more hydrophobic side of this helix, which faces away from helix $\alpha 5$, have more detrimental effects on the function of the protein than those facing helix $\alpha 5$.

An alternate explanation for the lower function of F150C and L181C is their position at the top of a helix. If helices $\alpha 5$ and $\alpha 6$ of Bcl-2 are inserted in the membrane, then the BH regions 1-3 are situated at the top of these helices. These regions are the “docking area” for interaction with the BH3 region of BH3-only pro-apoptotic proteins (Petros et al., 2004; Zha et al., 1997; Liu et al., 2003). Mutations to this area of Bcl-2 could disrupt the interaction between Bcl-2 and a BH3-only protein such as tBid. Studies using the point mutant Bcl-2 G145A have shown that a mutation to the BH1 domain results in loss of anti-apoptotic function (Yin et al., 1994). If Bcl-2 were binding to tBid to inhibit its pro-apoptotic function, then decreasing this interaction would cause Bcl-2 to be hypo-functional. Consistent with this notion, mutations lower in helix $\alpha 6$, further from this docking region, do not decrease function, as seen in mutant N172C.

Lower anti-apoptotic function of a mutant may also be due to degradation of the protein during etoposide or serum starvation treatment, an effect that is independent of baseline expression because of the dynamic nature of the membrane topology of Bcl-2. Thus, although the mutant may be stable in the tail anchored conformation in healthy cells, this may change after the change in conformation following the induction of

apoptosis. Unfortunately, data on Bcl-2 expression changes during apoptosis are not available, because the quantitative immunoblots were optimized for PARP detection to measure apoptosis, and Bcl-2 levels were too high to be detected in the linear range of the film under these conditions.

4.3 Change in Membrane Topology of Bcl-2 During Apoptosis

The model of topology which best fits the IASD labelling data is one in which Bcl-2, normally found as a single spanning membrane protein, changes conformation after the induction of apoptosis to become a polytopic membrane protein. In this conformation, helices $\alpha 5$ and $\alpha 6$ insert into and span the outer mitochondrial or microsomal membrane, causing residues in the loop between the helices to be present in the inter-membrane or luminal space (Figure 3.5c). Although this topology has been suggested previously in the literature and by our lab (Kim et al., 2004), this is the first report of the mapping of the region under two different apoptotic conditions in living cells.

Figure 3.5 indicates the location and pattern of protected and accessible residues in four schematic diagrams of Bcl-2. The discontinuous pattern of protected residues suggests that one side of each helix is in a hydrophobic environment whereas the other is in an aqueous environment. The helical wheel diagrams (Figure 3.5b) show the accessible residue in the middle of $\alpha 5$, V156C, on the same side of the helix as the charged residue E152C, opposite to protected residues such as C158 and G154C. The mutants on helix $\alpha 6$ which caused loss of function were on the more hydrophobic side of the helix opposite to

the accessible residues L175C and W176C and hydrophilic residues D171 and E179. If an aqueous central region were created between the helices after insertion into the membrane, residues facing this region would be close to each other. This is supported by the data in which mutations in residues on helix α_6 , in close proximity to and facing helix α_5 are more functional than those on the hydrophobic face of the helix.

Partial protection of a residue from labelling that was noted for a few of the mutants could be due to many reasons. If a cysteine residue is at the edge of the transmembrane region, it may fluctuate between being protected and accessible. For example, the partially protected cysteine at V159C is located at the bottom of helix α_5 between the protected position at I157C and the fully accessible residue N163C. The latter is in the loop between the two helices and is predicted to be in the inter-membrane space, therefore accessible to label. The partial protection of residue T178C in helix α_6 may be due to its position on the border between the aqueous face of the helix and the membrane protected face. Additional possibilities are discussed in the following section.

The labelling data from helix α_5 strongly supports this model of topology. The discontinuous pattern of protected residues supports the presence of an aqueous central area, encompassing E152 and V156, as well as an accessible loop between the helices at N163, S167 and P168. However, the labelling data of residues in helix α_6 is not as clear-cut. Unfortunately, three residues in the centre of helix α_6 do not contribute useful information to determine topology because these mutations resulted in little or no protein expression. Based on the helical wheel diagrams, the positions of these non-informative residues should be protected from labelling because of their central location within the

helix and the face on which they protrude. The labelling data from residues on opposing sides of helix $\alpha 5$, such as residues V156 and G154, show that while V156C was accessible, G154C was protected. The model would predict that corresponding residues on helix $\alpha 6$, such as L175 and M177 or W176 and A174, would also have the opposite labelling pattern.

Two hyper-functional mutant proteins exhibited partial protection of cysteine residues from IASD labelling during both treatment conditions. PARP cleavage data shows that at the time of labelling these cells were at an earlier stage of apoptosis. This suggests that although apoptosis was being inhibited, only a portion of the Bcl-2 in this sample had changed conformation. There are two possible explanations for these results: either a small number of these hyper-functional mutants in the polytopic conformation were sufficient to inhibit overall apoptosis or, inhibition of apoptosis was occurring without the conformational change. The possibility of two functional conformations of Bcl-2 will be discussed in the next section.

4.4 Functional Significance of the Change in Topology of Bcl-2 During Apoptosis

Consistent with our model indicating that the conformational change of Bcl-2 is associated with function, useful labelling data was obtained from mutants with anti-apoptotic function equal to or better than wild type. Furthermore, both hypo-functional and hyper-functional mutants did not fully undergo this conformational change.

Two mechanisms by which Bcl-2 inhibits apoptosis are by binding and sequestering BH3 region-only proteins, thereby indirectly preventing the activation of

Bax or Bak (Cheng et al., 2001; Thomenius et al., 2003) and by binding directly to Bax or Bak on the mitochondrial membrane to prevent oligomerization, pore formation and subsequent release of apoptotic mediators (Oltval et al., 1993; Wei et al., 2001; Zha et al., 1996a; Annis, 2004). Our data can reconcile these differences in the literature by suggesting a model in which Bcl-2 could perform both functions, but in different conformations. Bcl-2 can homodimerize, as shown in Figure 3.5d, as well as heterodimerize with other Bcl-2 proteins. During apoptosis Bax undergoes a change in topology similar to Bcl-2, in which central helices insert into the membrane thereby forming a pore (Annis et al., 2005). The similarity on the apoptotic membrane topologies of these two proteins would suggest that the central helices of Bcl-2 may bind to Bax in the membrane, inhibiting oligomerization. A Bcl-2/Bax heterodimer would have a similar topology to the Bcl-2 homodimer in Figure 3.5d, substituting helices $\alpha 5$, $\alpha 6$ and $\alpha 9$ of Bcl-2 for $\alpha 5$, $\alpha 6$ and $\alpha 9$ of Bax. This model of heterodimerization after conformational change is further supported by data from our lab generated by Dr Matt Annis, showing that over-expression of Bcl-2 in cells inhibits the formation of higher order oligomers of Bax, by forming heterodimers (Annis, 2004). Although the data presented here suggest Bcl-2 has at least two roles in inhibiting apoptosis, it is not clear whether the specific binding requirements of the two functions require different conformations, or if Bcl-2 inhibits both BH3-only proteins and Bax in the polytopic conformation.

Hyper-functional Bcl-2 mutants prevent apoptosis without going through the same conformational change as wild type. This suggests that the polytopic membrane conformation of Bcl-2 is not required for inhibition of BH3-only proteins, but may be

required for Bax inhibition. The mutations may markedly increase the affinity of Bcl-2 for BH3-only proteins before any change in conformation, thus decreasing the downstream activation of Bax or Bak. Cells expressing these mutants progress more slowly through apoptosis than wild type cells, thus experiments using longer treatment times before IASD labelling could be used to show whether these mutants retain the ability to change conformation. If no further conformational change occurs it would suggest that the anti-apoptotic activity of these mutants may be exclusively through BH3-only inhibition and does not require the polytopic conformation. Another possible mechanism of interaction is that the conformational change in Bcl-2 is induced after binding of BH3 proteins (Dlugosz et al., manuscript in preparation), and that hyper-functional mutants have enhanced allosteric regulation of this change.

Studies using hypo-functional mutants of Bcl-2 have given further insight into the two potential functional membrane topology of Bcl-2. The hypo-function seen in mutants such as E152C, L181C and V159D, may reflect their ability to perform only one of the anti-apoptotic functions of Bcl-2. Although the mutations may have damaged the ability to insert into the membrane, as discussed in previous sections, other characteristics such as the ability to interact with BH3-only proteins may have been retained. By only inhibiting BH3-only proteins, these mutants would be less effective than proteins that change conformation and perform both roles. In cells, the mutant V159D exists in dimers like wild type and inhibits tBid induced cytochrome c release from mitochondria *in vitro* almost as well as wild type (Dlugosz P, unpublished data), but in cells only a portion of the proteins undergo the conformational change after induction of apoptosis. This

suggests that V159D can interact with and inhibit tBid, but may not be able to oligomerize with Bax. The addition of a charged residue to the bottom of helix $\alpha 5$, in a position which is protected from IASD labelling by the membrane, may inhibit insertion.

Further investigation into characteristics of the hypo-functional mutant V159D and the hyper-functional G154A/G155A will increase our understanding of the role of Bcl-2 in apoptosis. The interaction between each mutant and Bax should be examined to determine if these mutants bind to Bax similar to wild type. Using isolated mitochondria from cells over expressing either V159D or G154A/G155A in co-immunoprecipitation studies with Bax (Dlugosz et al., manuscript in preparation) would show whether these mutants bind to Bax like wild type. However, the inability to bind Bax may not explain the decrease in apoptotic function. Studies investigating binding between Bcl-2 proteins shows the ability to hetero-oligomerize is necessary but not sufficient for apoptotic function. Removal of the BH4 region of Bcl-2 does not decrease Bcl-2/Bax or Bcl-2/BH3-only binding, but it does significantly decrease its anti-apoptotic function (Huang et al., 1998). In cells, perhaps this region is important for stabilization of the active conformation of Bcl-2. Alternatively, using cells over expressing either wild type Bcl-2, V159D or G154A/G155A, crosslinking studies could be designed to determine if Bcl-2 is in close proximity to Bax or BH3-only proteins during different stages of apoptosis. In addition, gel filtration experiments (Annis, 2004), could be done with mitochondria isolated from cells over expressing V159D or G154A/G155A after apoptosis has been induced. This would show whether either mutant could inhibit the formation of higher order oligomers of Bax, necessary for pore formation (Annis, 2004).

Further support for the dual role of Bcl-2 in apoptosis comes from research in our lab done by Lieven Billen using the closely related anti-apoptotic protein, Bcl-xL. Since Bcl-2 is difficult to purify, Bcl-xL is a better candidate for use in *in vitro* studies to investigate the interaction between anti-apoptotic and pro-apoptotic Bcl-2 members. Using a cell free system and mutant Bcl-2 family proteins, his data suggests that Bcl-xL can both sequester the BH3-only pro-apoptotic protein tBid, as well as inhibit the formation of higher order oligomerization of Bax in liposomes (Billen et al., manuscript in preparation). Additional research, from other labs, using Bcl-xL has shown that mobility and flexibility of the $\alpha 5$ and $\alpha 6$ helices are imperative to the anti-apoptotic function of the protein. Investigation into the hyper-functional mutant Bcl-xL Y22F/Q26N/R165K, referred to as Bcl-xFNK or Bcl-xL*, has shown that disruption of the hydrogen bonding between the pore forming $\alpha 5$ and $\alpha 6$ helices and the surrounding amphipathic helices in the cytosolic conformation dramatically increases the anti-apoptotic function of the protein (Asoh et al., 2000). This suggests that since increasing the mobility or flexibility of the putative environmentally sensitive transmembrane domain enhances function, a decrease would diminish it. Currently, in our lab we are constructing a mutant of Bcl-2, Bcl-2 S105C/E152C, referred to as Bcl-2*, designed to have a conditional di-sulfide bridge between helices $\alpha 5$ and $\alpha 2$. In cells, when the cysteine residues are oxidized, the flexibility of helices $\alpha 5$ and $\alpha 6$ would be drastically hindered, locking this mutant in the tail-anchored topology, rendering it unable to change conformation. Using mitochondria isolated from cells over-expressing this mutant, in the cell free assay described in (Dlugosz, 2004), we could test if this immobile area of the

protein could be induced to change conformation after the addition of a reducing agent, such as DTT, which would break the di-sulfide bridge, allowing Bcl-2 the necessary mobility in helices $\alpha 5$ and $\alpha 6$. If this protein is functional only after the di-sulfide bridge is disrupted, this would support to the functional significance of the membrane insertion of these helices. One potential problem with this mutant is that the single cysteine mutant E152C is hypo-functional, and thus the double mutant Bcl-2* may not be informative. Thus, additional conditional mutants may need to be designed to investigate this phenomenon.

4.5 Conclusion

Using cysteine scanning mutagenesis, I have shown that in the late stages of apoptosis Bcl-2 changes conformation from a single spanning membrane protein to a polytopic protein in which helices $\alpha 5$ and $\alpha 6$, in addition to helix $\alpha 9$, insert into and span the membrane. The labelling pattern of high and low functioning mutants suggests that this conformational change is functionally important for Bcl-2 to inhibit Bax from forming pro-apoptotic pores in the membrane. However this change may not be essential for partial anti-apoptotic function as Bcl-2 may be able to inhibit BH3-only proteins from its original tail-anchored conformation. Further studies investigating the conformation of Bcl-2 when actively inhibiting Bax and BH3-only proteins will demonstrate if Bcl-2 indeed has two active conformations.

CHAPTER 5: REFERENCES

Adams, J.M. and Cory, S. (2001). *Life-or-death decisions by the Bcl-2 protein family*. *Trends Biochem. Sci.* 26, 61-66.

Adams, M. and Cory, S. (1998). *The Bcl-2 Protein Family: Arbiters of Cell Survival*. *Science* 281, 1322.

Andrews, D. W. *Andrews Lab Manual*.

<http://www.science.mcmaster.ca/biochem/faculty/andrews/lab/projects/methodsandprograms/labman> . 2005.

Ref Type: Electronic Citation

Andrews, D.W., Lauffer, L., Walter, P., and Lingappa, V.R. (1989). *Evidence for a two-step mechanism involved in assembly of functional signal recognition particle receptor*. *J. Cell Biol.* 108, 797-810.

Annis, M. G. *Investigating the molecular mechanisms of Bcl-2 and Bax in the regulation of apoptosis*. 2004. McMaster University.

Ref Type: Thesis/Dissertation

Annis, M.G., Soucie, E.L., Dlugosz, P.J., Cruz-Aguado, J.A., Penn, L.Z., Leber, B., and Andrews, D.W. (2005). *Bax forms multispinning monomers that oligomerize to permeabilize membranes during apoptosis*. *EMBO J.*

Asoh, S., Ohtsu, T., and Ohta, S. (2000). *The super anti-apoptotic factor Bcl-xFNK constructed by disturbing intramolecular polar interactions in rat Bcl-xL*. *J. Biol. Chem.* 275, 37240-37245.

Bratton, S.B., MacFarlane, M., Cain, K., and Cohen, G.M. (2000). *Protein complexes activate distinct caspase cascades in death receptor and stress-induced apoptosis*. *Exp. Cell Res.* 256, 27-33.

Cande, C., Cecconi, F., Dessen, P., and Kroemer, G. (2002). *Apoptosis-inducing factor (AIF): key to the conserved caspase-independent pathways of cell death?* *J. Cell Sci.* 115, 4727-4734.

Cardone, M.H., Roy, N., Stennicke, H.R., Salvesen, G.S., Franke, T.F., Stanbridge, E., Frisch, S., and Reed, J.C. (1998). *Regulation of cell death protease caspase-9 by phosphorylation*. *Science* 282, 1318-1321.

Cheng, E.H., Wei, M.C., Weiler, S., Flavell, R.A., Mak, T.W., Lindsten, T., and Korsmeyer, S.J. (2001). *BCL-2, BCL-X(L) sequester BH3 domain-only molecules preventing BAX- and BAK-mediated mitochondrial apoptosis*. *Mol. Cell* 8, 705-711.

Chiarugi, A. and Moskowitz, M.A. (2002). *Cell biology. PARP-1--a perpetrator of apoptotic cell death?* *Science* 297, 200-201.

Cory,S. and Adams,J.M. (2002). *The Bcl2 family: regulators of the cellular life-or-death switch. Nat. Rev. Cancer* 2, 647-656.

Cory,S., Vaux,D.L., Strasser,A., Harris,A.W., and Adams,J.M. (1999). *Insights from Bcl-2 and Myc: malignancy involves abrogation of apoptosis as well as sustained proliferation. Cancer Res.* 59, 1685s-1692s.

Datta,S.R., Brunet,A., and Greenberg,M.E. (1999). *Cellular survival: a play in three Akts. Genes Dev.* 13, 2905-2927.

Datta,S.R., Dudek,H., Tao,X., Masters,S., Fu,H., Gotoh,Y., and Greenberg,M.E. (1997). *Akt phosphorylation of BAD couples survival signals to the cell-intrinsic death machinery. Cell* 91, 231-241.

Deveraux,Q.L., Schendel,S.L., and Reed,J.C. (2001). *Antiapoptotic proteins. The bcl-2 and inhibitor of apoptosis protein families. Cardiol. Clin.* 19, 57-74.

Diaz,J.L., Oltersdorf,T., Horne,W., McConnell,M., Wilson,G., Weeks,S., Garcia,T., and Fritz,L.C. (1997). *A common binding site mediates heterodimerization and homodimerization of Bcl-2 family members. J. Biol. Chem.* 272, 11350-11355.

Dlugosz, P. J. *Regulation of cytochrome c release by Bcl-2, Bax and tBid.* 2004. McMaster University.
Ref Type: Thesis/Dissertation

Du,C., Fang,M., Li,Y., Li,L., and Wang,X. (2000). *Smac, a mitochondrial protein that promotes cytochrome c-dependent caspase activation by eliminating IAP inhibition. Cell* 102, 33-42.

Evan,G.I., Wyllie,A.H., Gilbert,C.S., Littlewood,T.D., Land,H., Brooks,M., Waters,C.M., Penn,L.Z., and Hancock,D.C. (1992). *Induction of apoptosis in fibroblasts by c-myc protein. Cell* 69, 119-128.

Falcone,D. and Andrews,D.W. (1991). *Both the 5' untranslated region and the sequences surrounding the start site contribute to efficient initiation of translation in vitro. Mol. Cell Biol.* 11, 2656-2664.

Godbey,W.T., Wu,K.K., Hirasaki,G.J., and Mikos,A.G. (1999). *Improved packing of poly(ethylenimine)/DNA complexes increases transfection efficiency. Gene Ther.* 6, 1380-1388.

Guo,Y., Srinivasula,S.M., Druilhe,A., Fernandes-Alnemri,T., and Alnemri,E.S. (2002). *Caspase-2 induces apoptosis by releasing proapoptotic proteins from mitochondria. J. Biol. Chem.* 277, 13430-13437.

Gurevich,V.V., Pokrovskaya,I.D., Obukhova,T.A., and Zozulya,S.A. (1991). *Preparative in vitro mRNA synthesis using SP6 and T7 RNA polymerases. Anal. Biochem.* 195, 207-213.

Hande,K.R. (1998). *Clinical applications of anticancer drugs targeted to topoisomerase II. Biochim. Biophys. Acta* 1400, 173-184.

Ho, S.N., Hunt, H.D., Horton, R.M., Pullen, J.K., and Pease, L.R. (1989). Site-directed mutagenesis by overlap extension using the polymerase chain reaction. *Gene* 77, 51-59.

Huang, D.C., Adams, J.M., and Cory, S. (1998). The conserved N-terminal BH4 domain of Bcl-2 homologues is essential for inhibition of apoptosis and interaction with CED-4. *EMBO J.* 17, 1029-1039.

Huang, D.C., O'Reilly, L.A., Strasser, A., and Cory, S. (1997). The anti-apoptosis function of Bcl-2 can be genetically separated from its inhibitory effect on cell cycle entry. *EMBO J.* 16, 4628-4638.

Igney, F.H. and Krammer, P.H. (2002). Death and anti-death: tumour resistance to apoptosis. *Nat. Rev. Cancer* 2, 277-288.

Janiak, F., Leber, B., and Andrews, D.W. (1994). Assembly of Bcl-2 into microsomal and outer mitochondrial membranes. *J. Biol. Chem.* 269, 9842-9849.

Juin, P., Hunt, A., Littlewood, T., Griffiths, B., Swigart, L.B., Korsmeyer, S., and Evan, G. (2002). c-Myc functionally cooperates with Bax to induce apoptosis. *Mol. Cell Biol.* 22, 6158-6169.

Kerr, J.F., Wyllie, A.H., and Currie, A.R. (1972). Apoptosis: a basic biological phenomenon with wide-ranging implications in tissue kinetics. *Br. J. Cancer* 26, 239-257.

Kim, P.K., Annis, M.G., Dlugosz, P.J., Leber, B., and Andrews, D.W. (2004). During apoptosis bcl-2 changes membrane topology at both the endoplasmic reticulum and mitochondria. *Mol. Cell* 14, 523-529.

Krishnasastri, M., Walker, B., Braha, O., and Bayley, H. (1994). Surface labeling of key residues during assembly of the transmembrane pore formed by staphylococcal alpha-hemolysin. *FEBS Lett.* 356, 66-71.

Kroemer, G. and Reed, J.C. (2000). Mitochondrial control of cell death. *Nat. Med.* 6, 513-519.

Kuwana, T., Mackey, M.R., Perkins, G., Ellisman, M.H., Latterich, M., Schneider, R., Green, D.R., and Newmeyer, D.D. (2002). Bid, Bax, and lipids cooperate to form supramolecular openings in the outer mitochondrial membrane. *Cell* 111, 331-342.

Kyte, J. and Doolittle, R.F. (1982). A simple method for displaying the hydropathic character of a protein. *J. Mol. Biol.* 157, 105-132.

LaCasse, E.C., Baird, S., Korneluk, R.G., and MacKenzie, A.E. (1998). The inhibitors of apoptosis (IAPs) and their emerging role in cancer. *Oncogene* 17, 3247-3259.

Laemmli, U.K. (1970). Cleavage of structural proteins during the assembly of the head of bacteriophage T4. *Nature* 227, 680-685.

Li, L.Y., Luo, X., and Wang, X. (2001). Endonuclease G is an apoptotic DNase when released from mitochondria. *Nature* 412, 95-99.

- Littlewood, T.D., Hancock, D.C., Danielian, P.S., Parker, M.G., and Evan, G.I. (1995). A modified oestrogen receptor ligand-binding domain as an improved switch for the regulation of heterologous proteins. *Nucleic Acids Res.* 23, 1686-1690.
- Liu, X., Dai, S., Zhu, Y., Marrack, P., and Kappler, J.W. (2003). The structure of a Bcl-xL/Bim fragment complex: implications for Bim function. *Immunity.* 19, 341-352.
- Marsden, V.S., O'Connor, L., O'Reilly, L.A., Silke, J., Metcalf, D., Ekert, P.G., Huang, D.C., Cecconi, F., Kuida, K., Tomaselli, K.J., Roy, S., Nicholson, D.W., Vaux, D.L., Bouillet, P., Adams, J.M., and Strasser, A. (2002). Apoptosis initiated by Bcl-2-regulated caspase activation independently of the cytochrome c/Apaf-1/caspase-9 apoptosome. *Nature* 419, 634-637.
- Matsuyama, S., Schendel, S.L., Xie, Z., and Reed, J.C. (1998). Cytoprotection by Bcl-2 Requires the Pore-forming alpha 5 and alpha 6 Helices. *Journal of Biological Chemistry* 273, 30995-31001.
- Nakano, K. and Vousden, K.H. (2001). PUMA, a novel proapoptotic gene, is induced by p53. *Mol. Cell* 7, 683-694.
- Oda, E., Ohki, R., Murasawa, H., Nemoto, J., Shibue, T., Yamashita, T., Tokino, T., Taniguchi, T., and Tanaka, N. (2000). Noxa, a BH3-only member of the Bcl-2 family and candidate mediator of p53-induced apoptosis. *Science* 288, 1053-1058.
- Oltval, Z.N., Milliman, C.L., and Korsmeyer, S.J. (1993). Bcl-2 heterodimerizes in vivo with a conserved homolog, Bax, that accelerates programmed cell death. *Cell* 74, 609-619.
- Penninger, J.M. and Kroemer, G. (2003). Mitochondria, AIF and caspases--rivaling for cell death execution. *Nat. Cell Biol.* 5, 97-99.
- Petros, A.M., Medek, A., Nettesheim, D.G., Kim, D.H., Yoon, H.S., Swift, K., Matayoshi, E.D., Oltersdorf, T., and Fesik, S.W. (2001). Solution structure of the antiapoptotic protein bcl-2. *Proc. Natl. Acad. Sci. U. S. A* 98, 3012-3017.
- Petros, A.M., Olejniczak, E.T., and Fesik, S.W. (2004). Structural biology of the Bcl-2 family of proteins. *Biochim. Biophys. Acta* 1644, 83-94.
- Rosconi, M.P. and London, E. (2002). Topography of helices 5-7 in membrane-inserted diphtheria toxin T domain: identification and insertion boundaries of two hydrophobic sequences that do not form a stable transmembrane hairpin. *J. Biol. Chem.* 277, 16517-16527.
- Ryan, K.M., Phillips, A.C., and Vousden, K.H. (2001). Regulation and function of the p53 tumor suppressor protein. *Curr. Opin. Cell Biol.* 13, 332-337.
- Schendel, S.L., Montal, M., and Reed, J.C. (1998). Bcl-2 family proteins as ion-channels. *Cell Death. Differ.* 5, 372-380.
- Schendel, S.L., Xie, Z., Montal, M.O., Matsuyama, S., Montal, M., and Reed, J.C. (1997). Channel formation by antiapoptotic protein Bcl-2. *Proc. Natl. Acad. Sci. U. S. A* 94, 5113-5118.

Schmitz,I., Kirchhoff,S., and Kramer,P.H. (2000). Regulation of death receptor-mediated apoptosis pathways. *Int. J. Biochem. Cell Biol.* 32, 1123-1136.

Soucie,E.L., Annis,M.G., Sedivy,J., Filmus,J., Leber,B., Andrews,D.W., and Penn,L.Z. (2001). Myc potentiates apoptosis by stimulating Bax activity at the mitochondria. *Mol. Cell Biol.* 21, 4725-4736.

Susin,S.A., Lorenzo,H.K., Zamzami,N., Marzo,I., Snow,B.E., Brothers,G.M., Mangion,J., Jacotot,E., Costantini,P., Loeffler,M., Larochette,N., Goodlett,D.R., Aebersold,R., Siderovski,D.P., Penninger,J.M., and Kroemer,G. (1999). Molecular characterization of mitochondrial apoptosis-inducing factor. *Nature* 397, 441-446.

Thomenius,M.J. and Distelhorst,C.W. (2003). Bcl-2 on the endoplasmic reticulum: protecting the mitochondria from a distance. *J. Cell Sci.* 116, 4493-4499.

Thomenius,M.J., Wang,N.S., Reineks,E.Z., Wang,Z., and Distelhorst,C.W. (2003). Bcl-2 on the endoplasmic reticulum regulates Bax activity by binding to BH3-only proteins. *J. Biol. Chem.* 278, 6243-6250.

Tsujimoto,Y., Gorham,J., Cossman,J., Jaffe,E., and Croce,C.M. (1985). The t(14;18) chromosome translocations involved in B-cell neoplasms result from mistakes in VDJ joining. *Science* 229, 1390-1393.

Vaux,D.L., Cory,S., and Adams,J.M. (1988). Bcl-2 gene promotes haemopoietic cell survival and cooperates with c-myc to immortalize pre-B cells. *Nature* 335, 440-442.

Wang,X. (2001). The expanding role of mitochondria in apoptosis. *Genes Dev.* 15, 2922-2933.

Wattenberg,B. and Lithgow,T. (2001). Targeting of C-terminal (tail)-anchored proteins: understanding how cytoplasmic activities are anchored to intracellular membranes. *Traffic* 2, 66-71.

Wei,M.C., Lindsten,T., Mootha,V.K., Weiler,S., Gross,A., Ashiya,M., Thompson,C.B., and Korsmeyer,S.J. (2000). tBID, a membrane-targeted death ligand, oligomerizes BAK to release cytochrome c. *Genes Dev.* 14, 2060-2071.

Wei,M.C., Zong,W.X., Cheng,E.H., Lindsten,T., Panoutsakopoulou,V., Ross,A.J., Roth,K.A., MacGregor,G.R., Thompson,C.B., and Korsmeyer,S.J. (2001). Proapoptotic BAX and BAK: a requisite gateway to mitochondrial dysfunction and death. *Science* 292, 727-730.

Yang,J., Liu,X., Bhalla,K., Kim,C.N., Ibrado,A.M., Cai,J., Peng,T.I., Jones,D.P., and Wang,X. (1997). Prevention of Apoptosis by Bcl-2: Release of Cytochrome c from Mitochondria Blocked. *Science* 275, 1129.

Yin,X.M., Oltvai,Z.N., and Korsmeyer,S.J. (1994). BH1 and BH2 domains of Bcl-2 are required for inhibition of apoptosis and heterodimerization with Bax. *Nature* 369, 321-323.

Yu,J., Zhang,L., Hwang,P.M., Kinzler,K.W., and Vogelstein,B. (2001). PUMA induces the rapid apoptosis of colorectal cancer cells. *Mol. Cell* 7, 673-682.

Zha, H., Aime-Sempe, C., Sato, T., and Reed, J.C. (1996a). Proapoptotic protein Bax heterodimerizes with Bcl-2 and homodimerizes with Bax via a novel domain (BH3) distinct from BH1 and BH2. J. Biol. Chem. 271, 7440-7444.

Zha, J., Harada, H., Osipov, K., Jockel, J., Waksman, G., and Korsmeyer, S.J. (1997). BH3 domain of BAD is required for heterodimerization with BCL-XL and pro-apoptotic activity. J. Biol. Chem. 272, 24101-24104.

Zha, J., Harada, H., Yang, E., Jockel, J., and Korsmeyer, S.J. (1996b). Serine phosphorylation of death agonist BAD in response to survival factor results in binding to 14-3-3 not BCL-X(L). Cell 87, 619-628.

Zhang, Z., Lapolla, S.M., Annis, M.G., Truscott, M., Roberts, G.J., Miao, Y., Shao, Y., Tan, C., Peng, J., Johnson, A.E., Zhang, X.C., Andrews, D.W., and Lin, J. (2004). Bcl-2 homodimerization involves two distinct binding surfaces, a topographic arrangement that provides an effective mechanism for Bcl-2 to capture activated Bax. J. Biol. Chem. 279, 43920-43928.